

11-2018

## Sequestration Effect on the Open-Cyclic Switchable Property of Warfarin Induced By Cyclodextrin: Time-Resolved Fluorescence Study

Naji Saleh Ahmed Al-Dubaili

Follow this and additional works at: [https://scholarworks.uaeu.ac.ae/chem\\_theses](https://scholarworks.uaeu.ac.ae/chem_theses)

 Part of the [Chemistry Commons](#)

---

### Recommended Citation

Al-Dubaili, Naji Saleh Ahmed, "Sequestration Effect on the Open-Cyclic Switchable Property of Warfarin Induced By Cyclodextrin: Time-Resolved Fluorescence Study" (2018). *Chemistry Theses*. 5.  
[https://scholarworks.uaeu.ac.ae/chem\\_theses/5](https://scholarworks.uaeu.ac.ae/chem_theses/5)

This Thesis is brought to you for free and open access by the Chemistry at Scholarworks@UAEU. It has been accepted for inclusion in Chemistry Theses by an authorized administrator of Scholarworks@UAEU. For more information, please contact [fadl.musa@uaeu.ac.ae](mailto:fadl.musa@uaeu.ac.ae).



United Arab Emirates University

College of Science

Department of Chemistry

SEQUESTRATION EFFECT ON THE OPEN-CYCLIC  
SWITCHABLE PROPERTY OF WARFARIN INDUCED BY  
CYCLODEXTRIN: TIME-RESOLVED FLUORESCENCE STUDY

Naji Saleh Ahmed Al-Dubaili

This thesis is submitted in partial fulfilment of the requirements for the degree of  
Master of Science in Chemistry

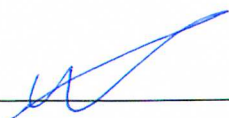
Under the Supervision of Dr. Na'il Saleh Ibrahim

November 2018

### Declaration of Original Work

I, Najji Saleh Ahmed Al-Dubaili, the undersigned, a graduate student at the United Arab Emirates University (UAEU), and the author of this thesis entitled "*Sequestration Effect on the Open-Cyclic Switchable Property of Warfarin Induced by Cyclodextrin: Time-Resolved Fluorescence Study*", hereby, solemnly declare that this thesis is my own original research work that has been done and prepared by me under the supervision of Dr. Na'il Saleh Ibrahim, in the College of Science at UAEU. This work has not previously been presented or published or formed the basis for the award of any academic degree, diploma or a similar title at this or any other university. Any materials borrowed from other sources (whether published or unpublished) and relied upon or included in my thesis have been properly cited and acknowledged in accordance with appropriate academic conventions. I further declare that there is no potential conflict of interest with respect to the research, data collection, authorship, presentation and/or publication of this thesis.

Student's Signature: \_\_\_\_\_



Date: 25/12/2018

## Approval of the Master Thesis


This Master Thesis is approved by the following Examining Committee Members:

- 1) Advisor (Committee Chair): Na'il Saleh Ibrahim

Title: Associate Professor

Department of Chemistry

College of Science

Signature 

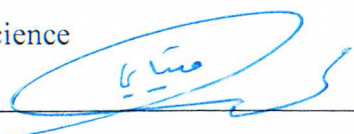
Date Dec 9, 2018

- 2) Member: Mohammed A. Meetani

Title: Associate Professor

Department of Chemistry

College of Science

Signature 

Date Dec 4 2018

- 3) Member (External Examiner): Nathir Al-Rawashdeh

*pf Thies Thiemann*

Title: Professor

Department of ETS, Math & Natural Science (Chemistry)

Institution: Higher Colleges of Technology, Ras Al Khaimah, UAE

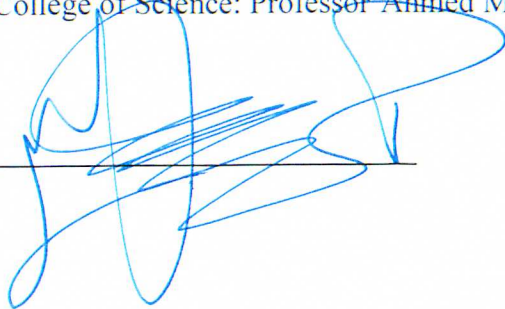
Signature 

Date Dec. 4, 2018

This Master Thesis is accepted by:

Dean of the College of Science: Professor Ahmed Murad

Signature

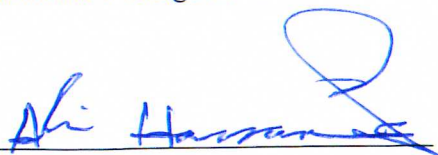


Date

24/12/2018

Acting Dean of the College of Graduate Studies: Professor Ali Hassan Al-Marzouqi

Signature



Date

17/1/2019

Copy 2 of 6

Copyright © 2018 Naji Saleh Ahmed Al-Dubaili  
All Rights Reserved

## **Advisory Committee**

1) Advisor: Na'il Saleh Ibrahim

Title: Associate Professor

Department of Chemistry

College of Science

2) Co-advisor: S. Salman Ashraf

Title: Professor

Department of Chemistry

College of Science

## Abstract

In this work, the photophysical properties of the fluorescent anticoagulant drug warfarin (W) were examined in water and inside methyl- $\beta$ -cyclodextrins (Me- $\beta$ -CD) through absorption and time-resolved fluorescence measurements at pH 3 and 9 and upon the selective excitation of different isomers of warfarin at 280 and 320 nm. The values of binding constants ( $2.9 \times 10^3 \text{ M}^{-1}$  and  $4.2 \times 10^2 \text{ M}^{-1}$  for protonated and deprotonated forms, respectively) were extracted from the spectrophotometric data. Both absorption and time-resolved fluorescence results established that the interior of the macromolecular host binds preferentially the open protonated form, red shifts the maximum of its absorption of light at  $\sim 305 \text{ nm}$ , extends its excited-state lifetime, and decreases its emission quantum yield ( $\Phi_F$ ). Collectively, sequestration of the open guest molecules decreases markedly their radiative rate constants ( $k_r$ ), likely due to formation of hydrogen-bonded complexes in both the ground and excited states. Due to lack of interactions, no change was observed in the excited-state lifetime of the cyclic form in the presence of Me- $\beta$ -CD. The host also increases the excited-state lifetime and  $\Phi_F$  of the drug deprotonated form (W<sup>-</sup>). These later findings could be attributed to the increased rigidity inside the cavity of Me- $\beta$ -CD. The  $pK_a$  values extracted from the variations of the UV-visible absorption spectra of W versus the pH of aqueous solution showed that the open isomer is more acidic in both ground and excited states. The positive shifts in  $pK_a$  values induced by three derivatives of cyclodextrins: HE- $\beta$ -CD, Ac- $\beta$ -CD, and Me- $\beta$ -CD supported the preferential binding of these hosts to open isomers over cyclic.

**Keywords:** open-cyclic tautomers, molecular switching, decay-associated spectra, warfarin, excited-state lifetime, cyclodextrins.



## Title and Abstract (in Arabic)

### تأثير تكوين معقدات داخل أوعية السيكلودكسترين على خاصية الانفتاح والانغلاق في دواء الوارفارين

#### الملخص

في هذا العمل ، تم فحص الخواص الفيزيائية الضوئية لعقار الوارفارين المضاد للتجلط الدموي في الماء وداخل الأوعية الجزيئية للميثيل-سيكلودكسترين (Me- $\beta$ -CD) من خلال قياسات الامتصاص والانبعث عند الرقم الهيدروجيني 3 و 9 الخاصة بايزومرات مختلفة من الوارفارين. تم استخلاص معاملات الارتباط ( $2.9 \times 10^3$  متر<sup>-1</sup> و  $4.2 \times 10^2$  متر<sup>-1</sup>) لأشكال حمضية وقاعدية مختلفة للعقار. أثبتت كل من نتائج الامتصاص والانبعثات الحركية أن الجزء الداخلي من المضيف يفضل الارتباط بالشكل الحمضي المفتوح ، مسببا امتصاص العقار لطاقة ضوئية أقل عند 305 ~ نانومتر ، وإطالة العمر الزمني للحالة المثارة ، كما يقلل من نسبة الانبعث ( $\Phi_F$ ). وبشكل عام إن الارتباط بواسطة جزيئات المضيف بالشكل ذو خاصية الانفتاح تقل بشكل ملحوظ من معاملات الإشعاع ( $k_r$ ) للدواء، ويرجع ذلك إلى تكوين روابط هيدروجينية في كل من الحالة المستقرة و المثارة.

**مفاهيم البحث الرئيسية:** التحول الجزيئي، الأطياف الحركية، زمن الحالة المثارة، أوعية السيكلودكسترين، وارفارين.

## **Acknowledgements**

I am deeply thankful and grateful to my advisor Dr. Na'il Saleh, who suggested this topic for me and who has been the driving force behind my motivation and the guidance in research to recover when my steps faltered. Also, I would like to express my sincere gratitude to my co-advisor Professor S. Salman Ashraf for his continuous optimism concerning this work, encouragement, enthusiasm, support and infinite patience throughout my Thesis.

I also owe a great debt of gratitude to the master program coordinator Professor Abbas Khaleel for his guidance, support, and assistance throughout my preparation of this thesis. It is a pleasure as well to thank all members of the Department of Chemistry at the United Arab Emirates University for assisting me all over my studies and research.

Finally, special deep appreciation is given to my family for providing me with unfailing support and encouragement that lead to this accomplishment.

## **Dedication**

*To my beloved parents and family*

## Table of Contents

Title .....	i
Declaration of Original Work .....	ii
Copyright .....	iii
Advisory Committee .....	iv
Approval of the Master Thesis .....	v
Abstract .....	vii
Title and Abstract (in Arabic) .....	viii
Acknowledgements .....	ix
Dedication .....	x
Table of Contents .....	xi
List of Tables.....	xiii
List of Figures .....	xiv
List of Abbreviations.....	xvi
Chapter 1: Introduction .....	1
1.1 Relevant Literature.....	1
1.1.1 Supramolecular Chemistry as a Science .....	1
1.1.2 Types of Molecular Containers (Hosts) .....	3
1.1.3 pK <sub>a</sub> of other drugs inside CBs and CDs .....	5
1.1.4 Biochemistry of Warfarin and its Importance.....	6
1.1.5 Warfarin as Fluorescent Probe .....	7
1.1.6 Time-Resolved Fluorescence .....	8
1.2 Aim of This Study.....	11
Chapter 2: Experimental Work .....	12
2.1 Reagents .....	12
2.2 Absorption/Steady-State Fluorescence Spectroscopy.....	12
2.3 pH-Titration Studies.....	13
2.4 Steady-State Binding Titration Studies.....	13
2.5 Time-Resolved Fluorescence Measurements.....	15
Chapter 3: Results & Discussion .....	16
3.1 Preliminary Investigation .....	16
3.2 Interactions of Warfarin with Cyclodextrins.....	19
3.2.1 Interactions of Warfarin with Ac- $\beta$ -CD at pH 3 .....	20
3.2.2 Interactions of Warfarin with Ac- $\beta$ -CD at pH 9 .....	21
3.2.3 Interactions of Warfarin with Me- $\beta$ -CD at pH 3.....	22

3.2.4 Interactions of Warfarin with Me- $\beta$ -CD at pH 9.....	23
3.3 Optical Measurements and Host-Induced p <i>K</i> <sub>a</sub> Shifts.....	24
3.4 Excitation, pH and Cyclodextrin Dependence of Warfarin Steady-State Fluorescence .....	29
3.5 Fluorescence Lifetime Measurements/Decay-Associated Spectra (DAS) .....	34
Chapter 4: Conclusion.....	42
4.1 Recommendations .....	43
References .....	44
Appendix .....	51

## List of Tables

Table 1: Major differences between CBs and CDs molecular containers .....	5
Table 2: Spectroscopic and photophysical data of W at 25 $\mu$ M in absence and in presence of Me- $\beta$ -CD (1.0 mM). The DAS maximum for each lifetime is given in bracket .....	35
Table 3: Fluorescence quantum yield $\Phi_F$ , Radiative rate constant $k_r$ , and Non-radiative rate constant $k_{nr}$ .....	39

## List of Figures

Figure 1: Self-assembly (a), self-sorting (b) and stimuli-responsiveness of supramolecular systems (c).....	1
Figure 2: Chemical structures of various derivatives of cyclodextrins (CDs) and cucurbiturils (CBs) molecular containers.....	3
Figure 3: Vitamin K cycle.....	7
Figure 4: Representative Jablonski diagram .....	9
Figure 5: Time-correlated single photon counting (TCSPC) diagram.....	10
Figure 6: Structural formulas of protonated warfarin (W): Keto-Enol tautomerism, deprotonated warfarin (W <sup>-</sup> ), and methyl- $\beta$ -cyclodextrins (Me- $\beta$ -CD) molecular container .....	11
Figure 7: UV-Visible absorption spectra at different pH values of W in Me- $\beta$ -CD with Ca <sup>+2</sup> .....	17
Figure 8: UV-Visible absorption spectra of W in aqueous solutions at different pH values from 2-10 in water and inside Me- $\beta$ -CD.....	17
Figure 9: UV-Visible absorption spectra at different pH values of W in Ac- $\beta$ -CD with Ca <sup>+2</sup> .....	18
Figure 10: UV-Visible absorption spectra of W in aqueous solutions at different pH values from 2-10 in water and inside Ac- $\beta$ -CD.....	18
Figure 11: The structures of selected $\beta$ -cyclodextrins macrocycles in the present work that were not studied before with W .....	19
Figure 12 : UV-Visible absorption titration of W (25 $\mu$ M) with Ac- $\beta$ -CD at pH 3.....	20
Figure 13: UV-Visible absorption titration of W (25 $\mu$ M) with Ac- $\beta$ -CD at pH 9.....	21
Figure 14: UV-Visible absorption titration of W (25 $\mu$ M) with Me- $\beta$ -CD at pH 3.....	22
Figure 15: UV-Visible absorption titration of W (25 $\mu$ M) with Me- $\beta$ -CD at pH 9.....	23
Figure 16: UV-Visible absorption spectra at different pH values of W in water.....	25
Figure 17: UV-Visible absorption spectra at different pH values of W in HE- $\beta$ -CD .....	25
Figure 18: UV-Visible absorption spectra at different pH values of W in Ac- $\beta$ -CD host .....	26
Figure 19: UV-Visible absorption spectra at different pH values of W in ME- $\beta$ -CD.....	26
Figure 20: UV-Visible absorption spectra of W in aqueous solutions at different pH values from 2-10 at $\lambda_{\text{abs}} = 280$ nm in water and inside HE- $\beta$ -CD, Ac- $\beta$ -CD, and Me- $\beta$ -CD .....	28

Figure 21: UV–Visible absorption spectra of W in aqueous solutions at different pH values from 2-10 $\lambda_{\text{abs}} = 305$ in water and inside HE- $\beta$ -CD, Ac- $\beta$ -CD, and Me- $\beta$ -CD.....	28
Figure 22: Fluorescence spectra of W (25 $\mu\text{M}$ ) at different pH values with excitation at 320 nm .....	30
Figure 23: Fluorescence spectra of W (25 $\mu\text{M}$ ) at different pH values with excitation at 280 nm .....	30
Figure 24: Fluorescence spectra of W (25 $\mu\text{M}$ ) at pH 2.5 and 10 with $\lambda_{\text{ex}} = 320$ nm and $\lambda_{\text{ex}} = 280$ nm as labeled by a distinct color.....	31
Figure 25: Fluorescence titration of W (25 $\mu\text{M}$ ) with Me- $\beta$ -CD at pH 9 with excitation at 320 nm the inset shows the corresponding titration curve and the 1:1 binding fit (solid line) with $K = (2.66 \pm 0.06) \times 10^2 \text{ M}^{-1}$ .....	32
Figure 26: Fluorescence spectra of W (25 $\mu\text{M}$ ) at pH 3 upon the addition of Me- $\beta$ -CD up to 250 $\mu\text{M}$ (10 equiv.) with $\lambda_{\text{ex}} = 320$ nm.....	33
Figure 27: Fluorescence spectra of W (25 $\mu\text{M}$ ) at pH 3 upon the addition of Me- $\beta$ -CD up to 250 $\mu\text{M}$ (10 equiv.) with $\lambda_{\text{ex}} = 280$ nm.....	33
Figure 28: Emission decays collected at 370 nm for W at 25 $\mu\text{M}$ in absence and in presence of Me- $\beta$ -CD (1.0 mM) upon exciting at 320 nm.....	36
Figure 29: Emission decays collected at 370 nm for W at 25 $\mu\text{M}$ in absence and in presence of Me- $\beta$ -CD (1.0 mM) upon exciting at 280 nm.....	36
Figure 30: Decay-associated spectra (DAS) of two-component mixture of fluorphores for W-Me- $\beta$ -CD host-guest complex (25 $\mu\text{M}$ for W and 1 mM for W-Me- $\beta$ -CD) at pH 3 upon exciting at 320 nm at room temperature .....	37
Figure 31: Decay-associated spectra (DAS) of two-component mixture of fluorphores for W-Me- $\beta$ -CD host-guest complex (25 $\mu\text{M}$ for W and 1 mM for W-Me- $\beta$ -CD) at pH 10 and upon exciting at 320 nm at room temperature .....	38
Figure 32: Collected emission decays measured over the emission spectrum of W at pH 3, excited at 320 nm from 330 to 490 nm every 10 nm with a dwell time of 50 s at each wavelength .....	51
Figure 33: Collected emission decays measured over the emission spectrum of W at pH 3, excited at 280 nm from 310 to 510 nm every 20 nm with a dwell time of 50 s at each wavelength .....	52
Figure 34: Collected emission decays measured over the emission spectrum of W-Me- $\beta$ -CD at pH 3 .....	53
Figure 35: Collected emission decays measured over the emission spectrum of W-Me- $\beta$ -CD at pH 3 .....	54
Figure 36: Collected emission decays measured over the emission spectrum of W at pH 9.....	55
Figure 37: Collected emission decays measured over the emission spectrum of W-Me- $\beta$ -CD at pH 9 .....	56



## List of Abbreviations

Ac- $\beta$ -CD	Acetyl- $\beta$ -cyclodextrins
DAS	Decay-associated spectra
G	Guest
H	Host
HE- $\beta$ -CD	(2-Hydroxyethyl)- $\beta$ -cyclodextrins
Me- $\beta$ -CD	Methyl- $\beta$ -cyclodextrins
TCSPC	Time-Correlated Single Photon Counting
W	Warfarin
$\alpha$ -CD	Alpha-cyclodextrins
$\beta$ -CD	Beta-cyclodextrins
$\gamma$ -CD	Gamma -cyclodextrins

## Chapter 1: Introduction

### 1.1 Relevant Literature

#### 1.1.1 Supramolecular Chemistry as a Science

Since its first development in 1987 by Lehn, Cram and Pedersen [1], supramolecular chemistry has been expanding into various applications, including biomedical applications [2], [3]. The host-guest concept involves non-covalent interaction of a guest (G) molecule inside the cavity of a host (H) molecule (Figure 1). These interactions include hydrogen-bonding interaction,  $\pi$ - $\pi$  stacking interaction, electrostatic interaction, van der Waals force, and hydrophobic/hydrophilic attraction [4].

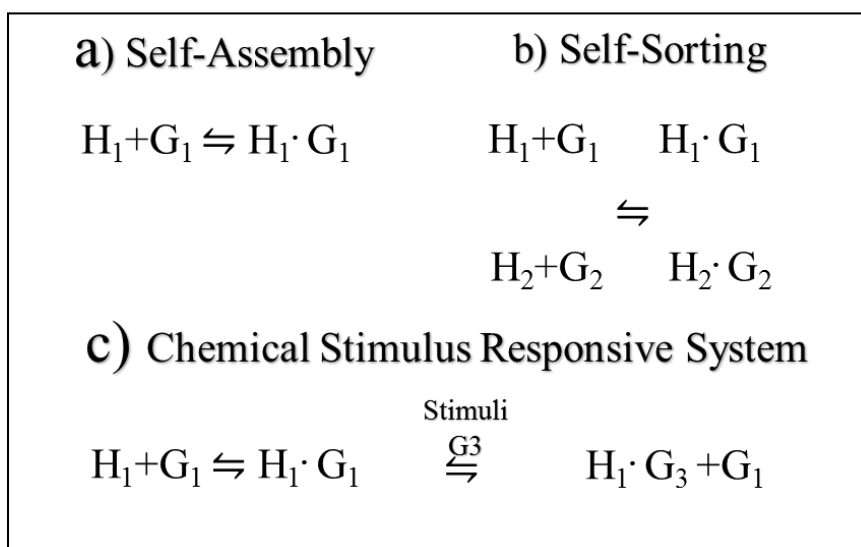


Figure 1: Self-assembly (a), self-sorting (b) and stimuli-responsiveness of supramolecular systems (c)

Figure 1 illustrates two important features of those non-covalent interactions: reversibility and responsiveness to external stimuli, such as pH, light, electrical

signal, heat, chemical competitor, etc. While self-assembly process (Figure 1a) describes transformation of small building blocks into one defined aggregate under certain conditions, self-sorting (Figure 1b) process is simultaneous occurrence of multiple self-assemblies into multiple well-defined aggregates under similar conditions. If building blocks of those self-assembling or self-sorting systems re-configured in responding to certain stimuli, the systems said to be stimuli-responsive systems (Figure 1c).

Supramolecular materials are naturally composed of two or more components that intrinsically self-assembled by non-covalent interactions. Such weak interactions inherently endow the materials with reversible, spontaneous assembly or disassembly feature, allowing convenient dissociation and reconstruction of the supramolecular systems at a low energy cost. Consequently, the “bottom-up” supramolecular approach has an adaptive capability in response to external stimuli that can trigger the self-assembly/disassembly equilibrium at the molecular level, leading into the design and fabrication of stimuli-responsive functional, smart materials for various applications, such as in biomedicine [5].

When compared to routine covalent modifications, the non-covalent method considered inexpensive and environmentally safe approach. On the one hand, it bypasses the burdens in multiple organic synthesis steps [6], and on the other it may combine already existing products in the market, whose safety and low-toxicity have been already confirmed [7], [8]. The low toxicity, in particular, motivated more researchers to utilize supramolecular systems in biological field as bio-inspired materials [9], [10].

### 1.1.2 Types of Molecular Containers (Hosts)

There have been several host-guest systems reported in aqueous solution for biomedical applications with stimuli-responsive abilities [11]. Cyclodextrins (CDs) [12] and Cucurbit[n]uril (CBs) [13] are examples of hosts that bind with the guest by noncovalent interactions as illustrated in Figure 2.

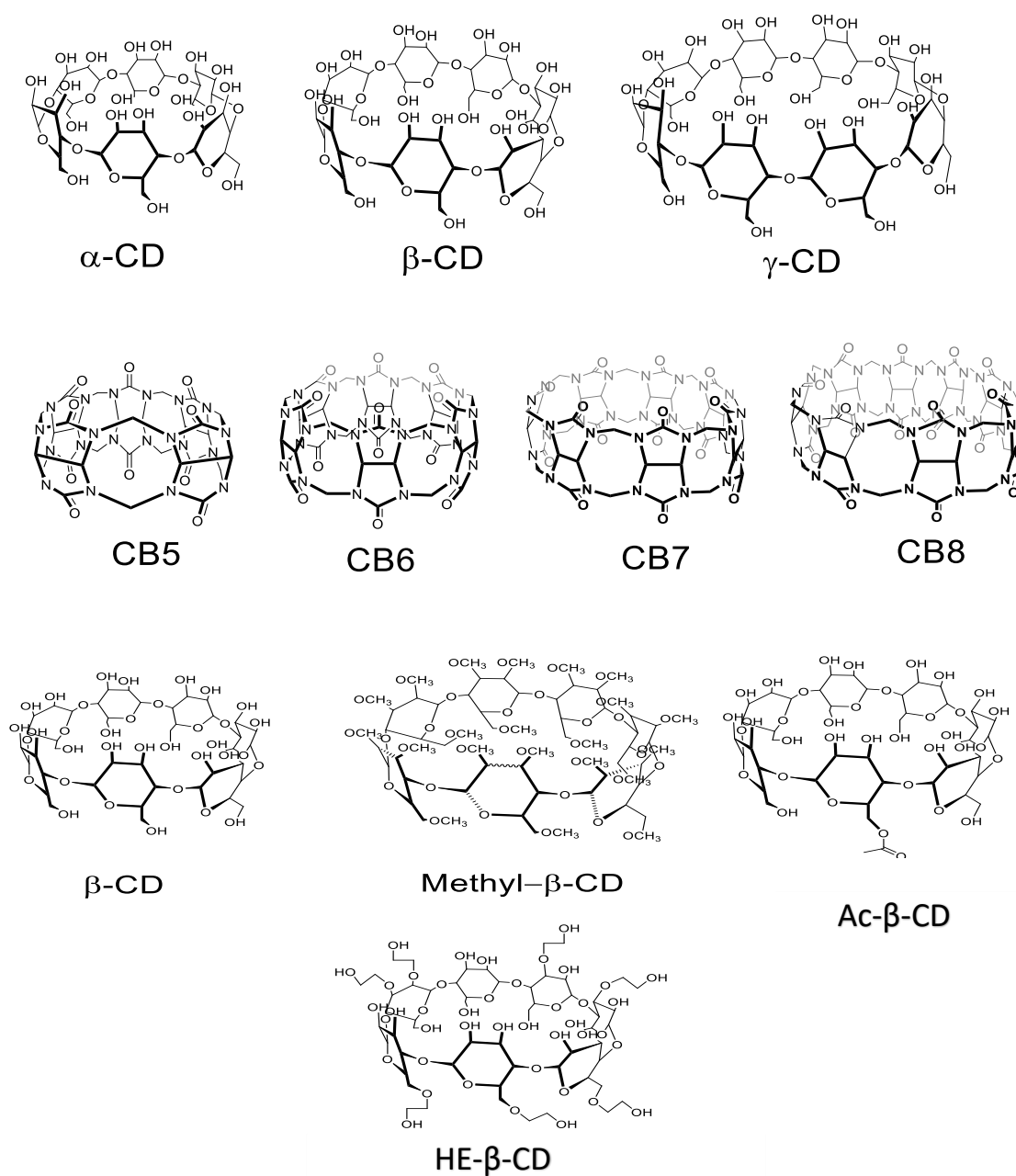


Figure 2: Chemical structures of various derivatives of cyclodextrins (CDs) and cucurbiturils (CBs) molecular containers

Table 1 summarizes some features that distinguish the two type of containers CDs and CBs. For example, CBs have much higher affinity to bind guest molecules [2]. For instance, the binding constant ( $K$ ) for CDs-based host–guest complexes can reach  $10^4 \text{ M}^{-1}$  [12], [14], [15], and that for CBs-based host–guest complexes can be as high as  $10^{15} \text{ M}^{-1}$  [16]. Another important feature is the distinct carbonyl group, which is responsible for the binding between CBs and cationic guests through ion-dipole interactions, leading to an increase in their acid-dissociation constant [17].

However the important feature of CDs is their ability to increase the solubility of poorly soluble drugs [12], [14], [15]. CDs consist of ( $\alpha$ -1,4-)-linked  $\alpha$ -D-glucopyranose units with a hydrophobic central cavity which gives CDs the cones shape with the hydrophilic outer surface [12], [14], [15]. There are three main types of CDs ( $\alpha$ ,  $\beta$  and  $\gamma$ ), the difference between them is the number of glucopyranose units in their structures which is six, seven and eight, respectively [12], [14], [15].

On the other hand, CBs composed of glycoluril units connected by methylene groups. The isolation of major CBs members was achieved only 80 years after its first synthesis in acidic media. By the year 2000, all members of CBs from 1-10 were isolated except CB9 (i.e., CB5, CB6, CB7, CB8, and CB10) [18]–[20]. In 2015, CB14 was isolated [21].

Table 1: Major differences between CBs and CDs molecular containers

	<b>CBs</b>	<b>CDs</b>
Binding constant	$10^{15} \text{ M}^{-1}$	$10^4 \text{ M}^{-1}$
Features	carbonyl group and ion-dipole interactions ( <b>increase <math>pK_a</math></b> of guests)	<b>increase the solubility</b> of insoluble guests
Structure	composed of glycoluril units connected by methylene groups with a hydrophobic cavity	Composed of glucopyranose units with a hydrophobic cavity
Types	CB5, CB6, CB7, CB8, CB10, and CB14	$\alpha$ , $\beta$ and $\gamma$ and derivatives thereof

### 1.1.3 $pK_a$ of other drugs inside CBs and CDs

In general, inclusion of guest molecules inside CDs and CBs changes their physical and chemical properties. Also, CDs prefer to bind the neutral forms of guests over their cationic forms, consequently, this will induce negative  $pK_a$  shift of guest molecules [2], [22]–[24]. On the other hand, CBs will induce positive  $pK_a$  shift of guest molecules because it favors binding the protonated form rather than the neutral form [25]–[27]. The host-induced  $pK_a$  shift was related to the carbonyl groups of CBs that are partially negatively charged [2], [25], [28]–[31].

For example, Saleh *et al.* studied the encapsulation of benzimidazoles [26], [32] which are commercial fungicides [33], [34] with CB7. The inclusion affects the  $pK_a$  of the benzimidazoles and leads to positive  $pK_a$  shift. This is equivalent to say that, CB7 has stabilized the protonated form of benzimidazole guest molecule,

increasing its solubility [26]. In another example, the interaction of CB7 with tropicamide which is an ocular drug; whose  $pK_a$  is 5.4 was also examined [35], [36]. Encapsulation of tropicamide with CB7 and CB8 increases the  $pK_a$  by (0.5 and 1.5) units respectively. As a result, the ionization degree of the drug was enhanced, which is of relevant to drug bioavailability [35].

From a different prospective, inclusion of drugs inside CDs and CBs has not only induced  $pK_a$  shift but also increased the fluorescence of these drugs [31], [35]. Koner *et al.* studied the encapsulation of dapoxyl sodium sulfonate (DSS) with  $\alpha$ - and  $\beta$ -cyclodextrins. Not only a 0.8 negative  $pK_a$  shift was noticed due to encapsulation of DSS inside  $\beta$ -cyclodextrins, but also the emission of the DSS was consequently increased significantly [37].

#### **1.1.4 Biochemistry of Warfarin and its Importance**

Warfarin is an oral anticoagulant drug that is widely used for a patient who has cardiovascular disease [38]. The mechanism of how warfarin prevents blood from clotting is shown in Figure 3 [39], which illustrates Vitamin K cycle. Warfarin reduces the production of clotting factors II, VII, IX and X, and the anticoagulant proteins C and S. This could happen by inhibiting the enzyme, Vitamin K epoxide reductase, that is required to reproduce vitamin K epoxide in the reduced form. Reduced vitamin K<sub>1</sub> (vitamin K<sub>1</sub>H<sub>2</sub>) is required as cofactor for  $\gamma$ -carboxylase to converts glutamic acid (Glu) residues to  $\gamma$ -carboxyglutamic acid (Gla) by adding CO<sub>2</sub>, which is needed to induce blood clotting [39].

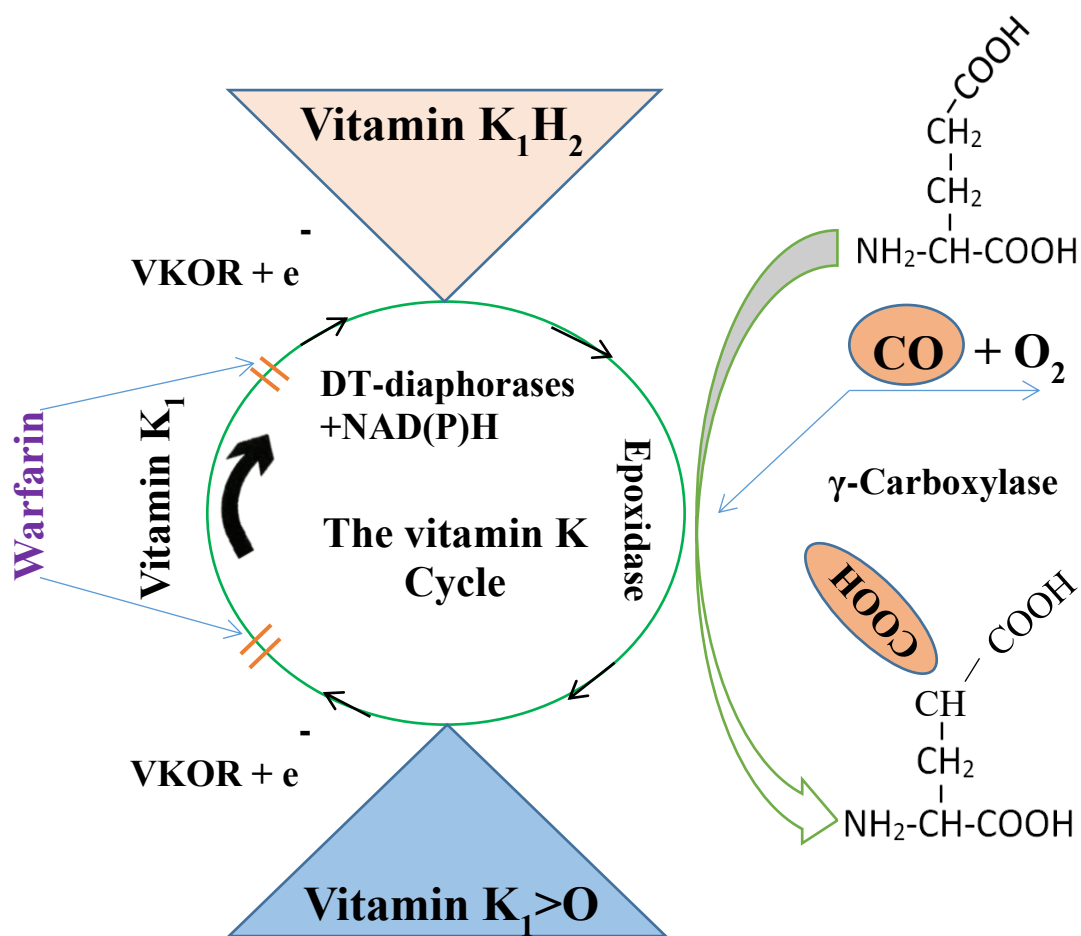


Figure 3: Vitamin K cycle

### 1.1.5 Warfarin as Fluorescent Probe

The fluorescence properties of warfarin which is a coumarin derivative [40] have attracted attention for several decades. Like other fluorescent probes, coumarins display photophysical properties that are sensitive to their local environments, such as supramolecular host cavities [41]. Within this context, supramolecular host-guest approach alongside fluorescence behavior of new coumarin derivative was exploited by Saleh *et al.* towards molecular recognition of optically inactive analytes [42].



There have been number of studies on the structures of W in different solvents and at different pH by NMR, absorption and time-resolved fluorescence [43]–[46]. The early precedent reports described structures of drug in solution [43], [44] to be present at pH lower than its  $pK_a \sim 5$  as either open or cyclic protonated form and at pH higher than its  $pK_a$  as deprotonated form, whose side chain is open. In addition to that, photophysical properties of W in different solvents and solvent mixtures were profoundly examined [45], [46].

### **1.1.6 Time-Resolved Fluorescence**

One of the most powerful tools for investigating the physical and chemical properties of matter or biological systems is the time-resolved fluorescence spectroscopy [47]. This becomes essential in light of the fact that steady state emission spectra sometimes are unspecified because the overlap emission profile of different fluorophores. In addition, steady-state fluorescence spectroscopy is not quantitative due to bleaching effects and gives no information in relation to the rate of deactivation process of an excited state of a drug molecule, as summarized by the Jablonski diagram in Figure 4 [48].

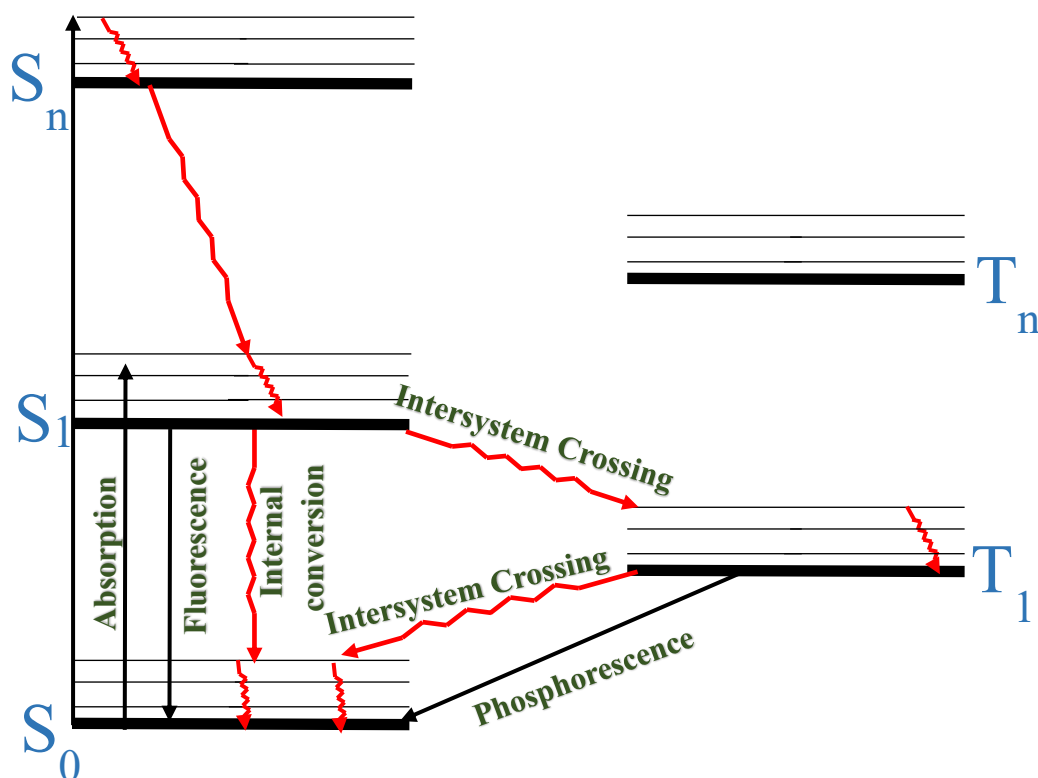


Figure 4: Representative Jablonski diagram

### 1.1.6.1 Time-Correlated Single Photon Counting (TCSPC)

One of the most popular ways of measuring time-resolved fluorescence is (TCSPC). The principle of this method is illustrated in Figure 5 [48]. A molecule will be excited by a laser pulse, a beam splitter is used to split part of the laser light which will reach to the photodiode. The photodiode is responsible for forming an electrical pulse that will be converted to ‘start’ signal by the discriminator. However, the stop signal is produced from the photon emitted by the sample that is recorded by a photomultiplier. The start signal is then required to start the time-to-amplitude converter (TAC).

TAC is the most important part of the TCSPC technique because of its role, which is measuring the difference in time between the start and stop signals that are proportional to the analogue voltage signal. Consequently, the voltage that produced by TAC is stored in a multi-channel analyzer [48].

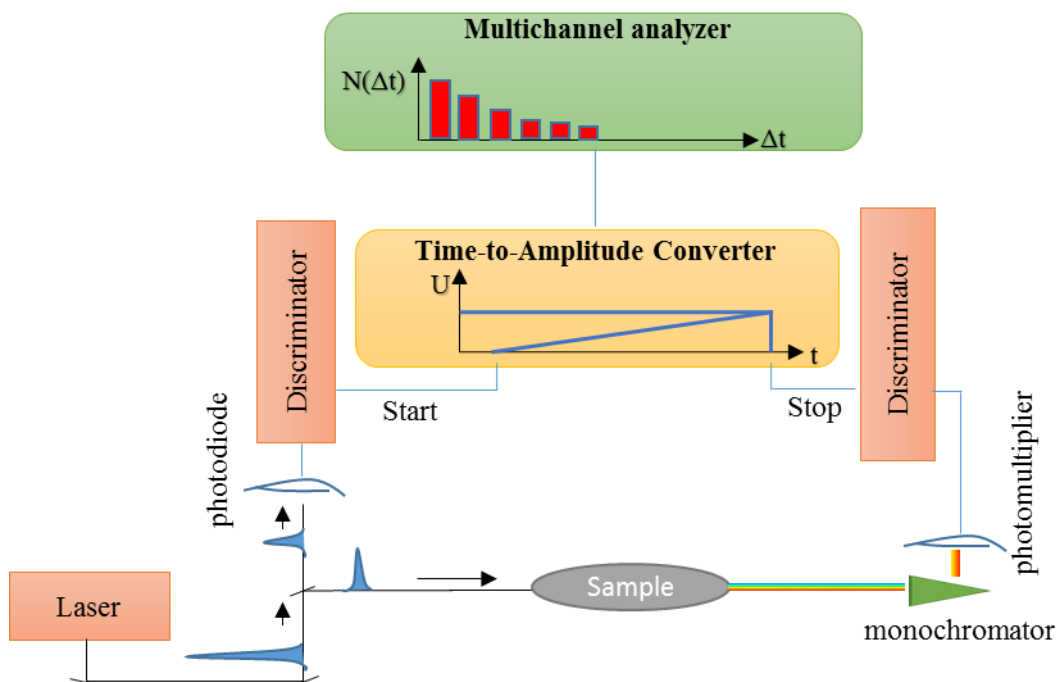


Figure 5: Time-correlated single photon counting (TCSPC) diagram

## 1.2 Aim of This Study

Our goal is to characterize the photophysical behaviors of warfarin (W) inside cyclodextrin macrocycles as shown in (Figure 6). In previous work, steady-state fluorescence measurements were studied. However, to understand the effect of encapsulation of warfarin on emission, a more quantitative tool for examining the effects of supramolecular cavities is needed. Accordingly, measurements of fluorescence lifetimes of W in presence and absence of cyclodextrins are highly motivated in the present work.

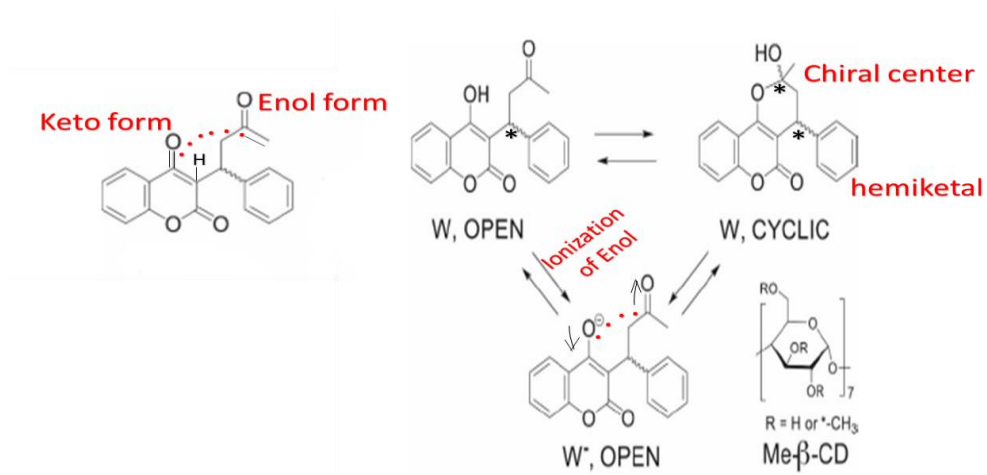


Figure 6: Structural formulas of protonated warfarin (W): Keto-Enol tautomerism, deprotonated warfarin (W<sup>-</sup>), and methyl-β-cyclodextrins (Me-β-CD) molecular container

## Chapter 2: Experimental Work

### 2.1 Reagents

Wafarin (W), Acetyl- $\beta$ -cyclodextrins (Ac- $\beta$ -CD), Methyl- $\beta$ -cyclodextrins (Me- $\beta$ -CD), and (2-Hydroxyethyl)- $\beta$ -cyclodextrins (HE- $\beta$ -CD) were purchased from Sigma-Aldrich Chemie GmbH, Taufkirchen, Germany (purity 99 %). D<sub>2</sub>O, DCl and NaOD were also purchased from Sigma-Aldrich. Millipore water had conductivity less than 0.05  $\mu$ S. The pH values of the solutions were adjusted ( $\pm$  0.2 units) by adding adequate amounts of HCl or NaOH.

### 2.2 Absorption/Steady-State Fluorescence Spectroscopy.

The UV/Visible absorption spectra were measured on Cary-300 instrument (Agilent) at room temperature, between 200 and 500 nm. Fluorescence spectra measurements were scanned at room temperature, between 300 and 550 nm on a Cary-Eclipse fluorimeter. Slit widths were 5 nm for both excitation and emission monochromators, unless otherwise specified. pH values were recorded using a pH meter (WTW 330i equipped with a WTW SenTix Mic glass electrode). Quartz cuvettes (1.0 cm, 3.0 mL) were used in all spectroscopic measurements and were obtained from Starna Cells Inc. (Atascadero, CA).

### 2.3 pH-Titration Studies

The pH titration by UV–Visible absorption spectroscopic method was accomplished by measuring the pH values of about 3 ml solutions contained in a rectangular quartz cuvette with 1 cm optical path length, and the absorption spectra were then recorded. To adjust pH, microliter volumes from 0.01 and 0.1M NaOH solution were pipetted consecutively to achieve the indicated pH values. The  $pK_a$  value was finally determined from fitting the titration data at a selected wavelength to sigmoidal formula derived from Henderson-Hasselbalch and Beer-Lambert laws. The fitting algorithm was provided by SigmaPlot's software (version 6.1; SPCC, Inc., Chicago, Illinois, USA).

### 2.4 Steady-State Binding Titration Studies

In the titration experiment, the total concentrations of the W were kept constant and that of the host was gradually increased. The pH of a certain volume of H<sub>2</sub>O was first adjusted to either ~3 or ~9 in which a stock solution of W was prepared to give a final concentration of ~25  $\mu$ M. A calculated weight of  $\beta$ -CD derivatives was added to the same solution of W to prepare the stock solution of the complex (~ 3.5 mM). The solutions with the final concentration of  $\beta$ -CD were prepared by gradually adding increment volumes of the complex's stock solution to 2.4 ml of the free W directly in the quartz cuvettes. The absorption or fluorescence spectra were measured for each solution. The signals at certain wavelength were plotted as a function of host's total concentrations. The intermolecular interaction between  $\beta$ -CD and W may be quantified by the affinity constant referred to as the association equilibrium (K):



$$K = \frac{[W\text{-}\beta\text{-CD}]}{[W][\beta\text{-CD}]} \quad (2)$$

$$C_W = [W] + [W\text{-}\beta\text{-CD}] \quad (3)$$

$$C_{\beta\text{-CD}} = [\beta\text{-CD}] + [W\text{-}\beta\text{-CD}] \quad (4)$$

Where  $C_W$  and  $C_{\beta\text{-CD}}$  mean the total concentrations of W and  $\beta\text{-CD}$ , respectively. It can be written that:

$$Y \text{ (Reading at certain } \lambda) = \text{constant 1} * [W] + \text{constant 2} * [W\text{-}\beta\text{-CD}] \quad (5)$$

Using Eqs.(2)-(5), we obtain

$$\Delta Y = \frac{\Delta(\text{constant})C_{\beta\text{-CD}}}{\frac{2}{KC_W - 1 - KC_{\beta\text{-CD}} + \sqrt{(1 - KC_W + KC_{\beta\text{-CD}})^2 + 4KC_W}} + 1} \quad (6)$$

Where  $\Delta Y$  = optical changes at a given  $\lambda$ ;  $\Delta(\text{constant})$ = the difference between the molar absorptivity of free and  $\beta\text{-CD}$ -complexed W in the case of absorption titration, and  $K$  = binding constant. The binding constants ( $K$ ) were then evaluated by using the nonlinear formula of Eq. (6). Constant 2 was left as a floating parameter in the analysis by Levenberg-Marquardt algorithm, which was provided by SigmaPlot's software.

## 2.5 Time-Resolved Fluorescence Measurements

The emission decays of W in absence and presence of Me- $\beta$ -CD at different pH values were collected using LifeSpec II spectrometer that is based on TCSPC method with excitation at 280 and 320 nm using two Edinburgh diode lasers with repetition rate at 20 MHz, time resolution of 90 ps, and a red-sensitive high-speed PMT detector (Hamamatsu, H5773-04). Emission decay were collected every 10 nm over the entire emission spectra of W and W- $\beta$ -CD complex in aqueous solution with a dwell time of 50 s at each wavelength. The data were globally fitted to mono-exponential and bi-exponential model functions depending on the tested sample, then convoluted with instrument response function (IRF) of ~90 ps. The time-resolved data were specifically analyzed using Edinburgh FAST software (Appendix) in which decay-associated spectra (DAS) were constructed from the extracted intensity-contribution fraction ( $f_i$ ) calculated from the pre-exponential amplitudes ( $B_i$ ), as follows:

$$I(t) = \sum_i B_i \exp(-t/\tau_i) \quad (7)$$

$$f_i = \frac{B_i \tau_i}{\sum_j B_j \tau_j} \quad (8)$$

$\tau$ : lifetime for each electronic state (species)

Target analysis utilizing Glotaran software<sup>11</sup> were performed to confirm the kinetic expression for the population transfer of the two excited states that belong to free and CD-complexed W. Results indicated two mono-exponentially in parallel, which validates the meaning of DAS as described in text.



## Chapter 3: Results & Discussion

### 3.1 Preliminary Investigation

At the beginning of this work, the establishment of reversible and stimuli-responsiveness host-guest complexes to calcium ions in aqueous solutions was pursued. The reversibility in drug retention and release can be achieved in response to the added calcium ions to different host-guest complexes of warfarin with cyclodextrins. While the drug causes blood bleeding, addition of calcium would then replace the drug from the cavity of host, inducing blood clotting [39]. Our envisaged results are inspired by recent reports [26], [37] on the possibility of reversibly tune the binding affinity of the guest to different hosts utilizing host-induced  $pK_a$  shifts which is accompanied by modulation of fluorescence signal.

Collectively, our focus was on creating a balance between blood bleeding and blood clotting that could be utilized in blood cells in the future while being monitored online by emission signal. The inspiration specifically comes from the ability of carbonyl-containing containers (see Ac- $\beta$ -CD Figure 2) to tune the  $pK_a$  values of the embedded guests due to ion-dipole interaction.

Unfortunately, as shown in Figures 7-10 the  $pK_a$  shift is less than 1 unit between Warfarin and CDs. As a result, monitoring the stimuli responsiveness to calcium becomes impractical under these conditions. Alternatively, we opted to pursue the photochemistry of warfarin in water and inside CD with a similar aim towards establishing stimuli-responsive, reversible system yet due to the ability of host to induce molecular switching instead of  $pK_a$  shifts.

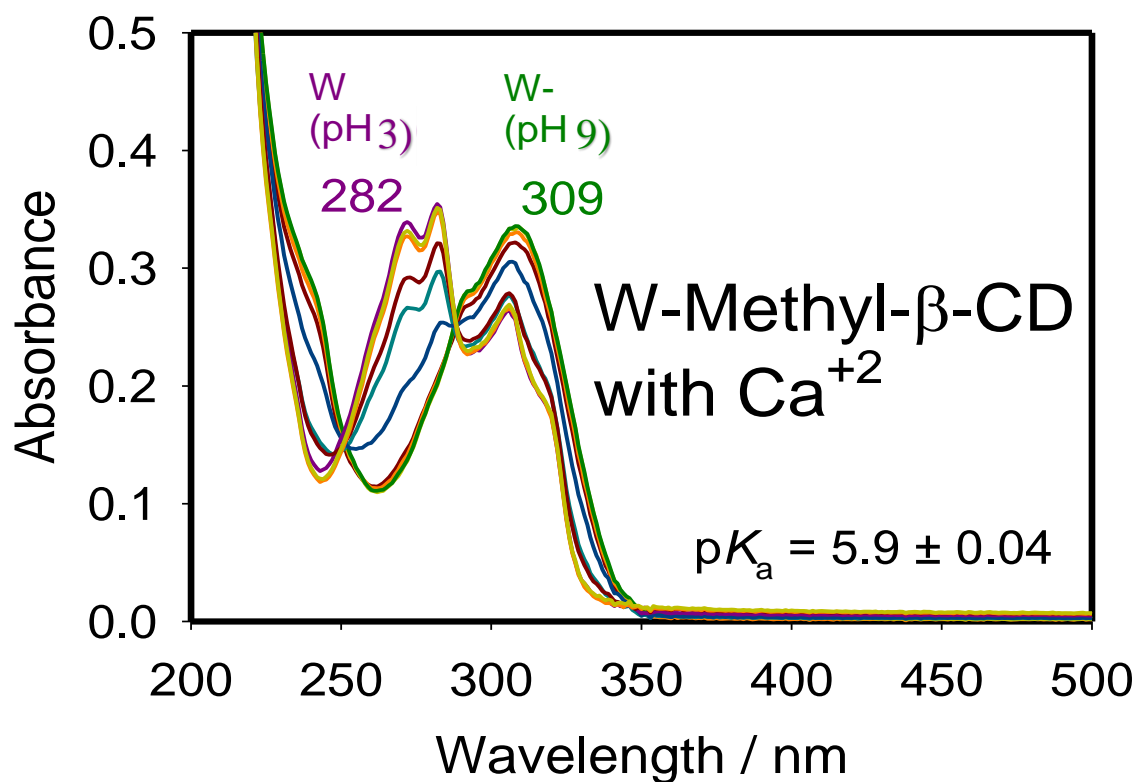


Figure 7: UV-Visible absorption spectra at different pH values of W in Me- $\beta$ -CD with  $\text{Ca}^{+2}$

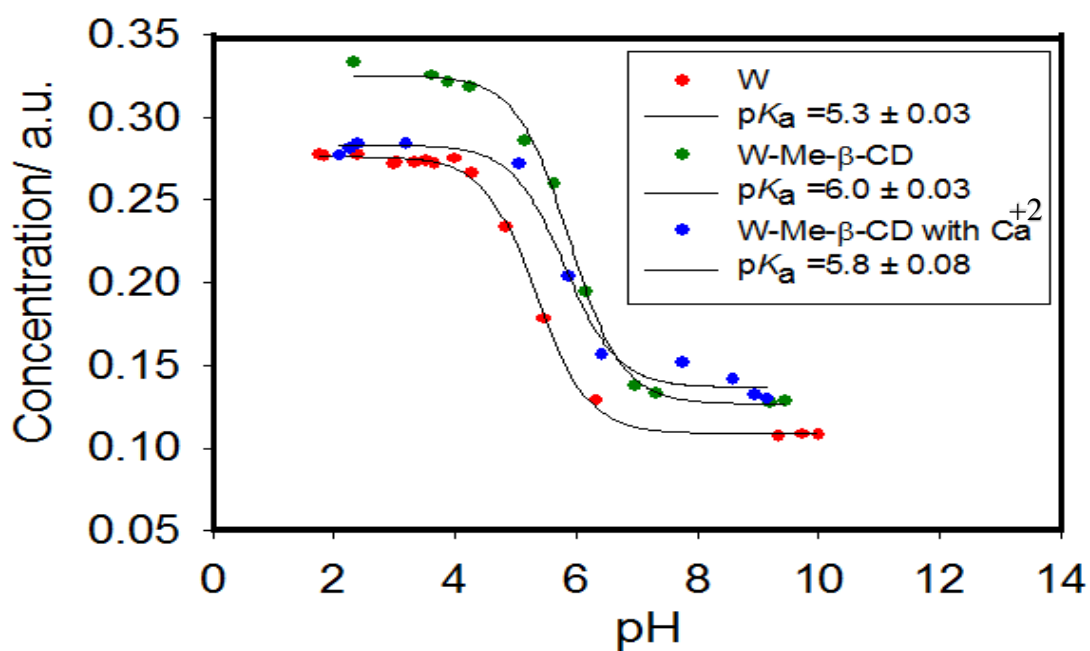


Figure 8: UV-Visible absorption spectra of W in aqueous solutions at different pH values from 2-10 in water and inside Me- $\beta$ -CD. The experimental fitting error for the indicated  $\text{p}K_a$  values and the corresponding spectra are shown in the insets

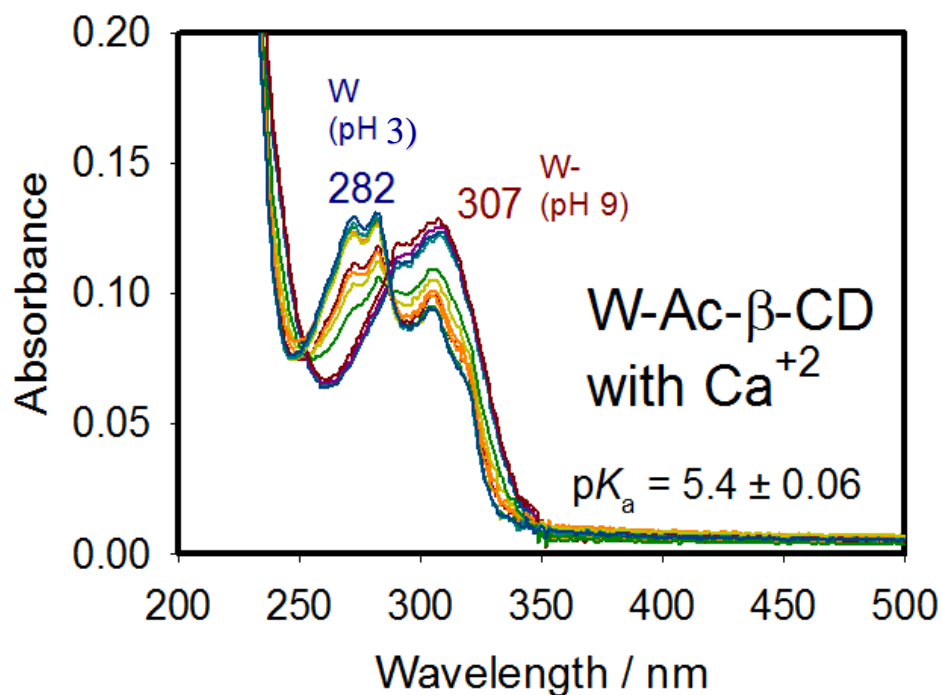


Figure 9: UV-Visible absorption spectra at different pH values of W in Ac- $\beta$ -CD with  $\text{Ca}^{+2}$

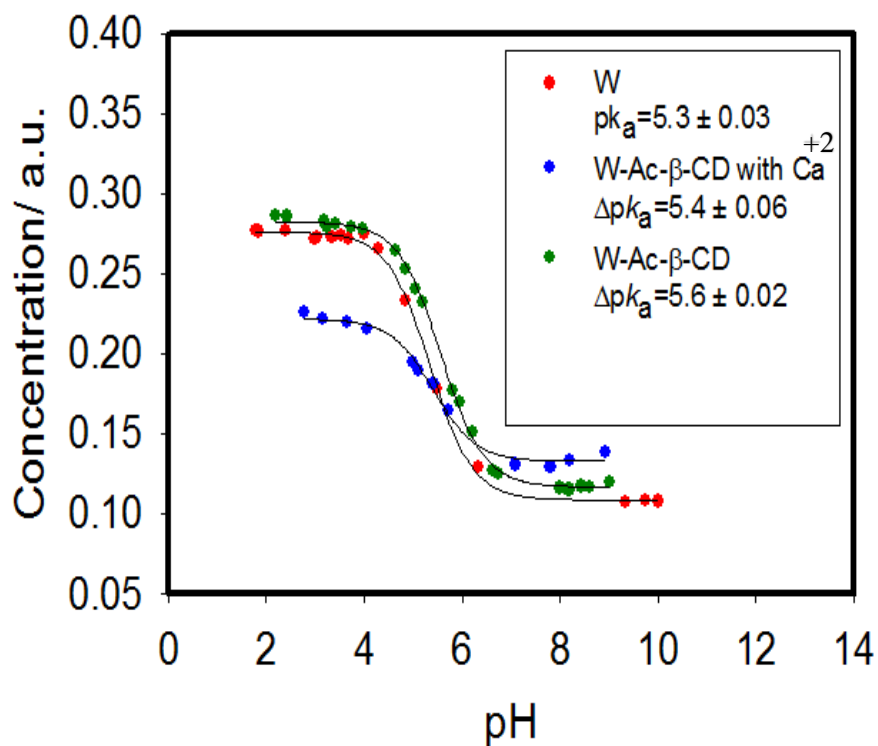


Figure 10: UV-Visible absorption spectra of W in aqueous solutions at different pH values from 2-10 in water and inside Ac- $\beta$ -CD. The experimental fitting error for the indicated  $pK_a$  values and the corresponding spectra are shown in the insets

### 3.2 Interactions of Warfarin with Cyclodextrins

Precedent reports on the interactions of W with several derivatives of CDs [46], [49], [38], [50] have been considered in planning the experiments in this work. Figure 11 shows new derivatives of  $\beta$ -CD were pursued, namely Acetyl- $\beta$ -CD and 2-Hydroxyl Ethyl- $\beta$ -CD.

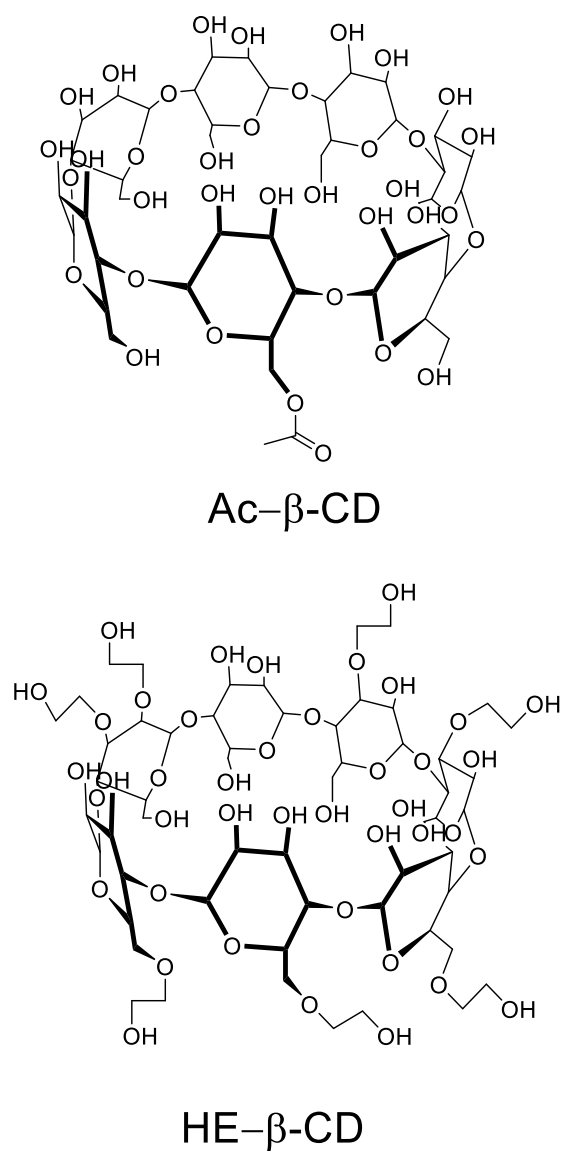


Figure 11: The structures of selected  $\beta$ -cyclodextrins macrocycles in the present work that were not studied before with W

### 3.2.1 Interactions of Warfarin with Ac- $\beta$ -CD at pH 3

The rationale behinds our selection arises from the presence of additional hydroxyl or carbonyl functional groups that could enhance interaction with W. Unfortunately, Ac- $\beta$ -CD cyclodextrin at pH 3 gave weak or no interaction with W, as monitored by UV-Visible absorption measurements in Figure 12.

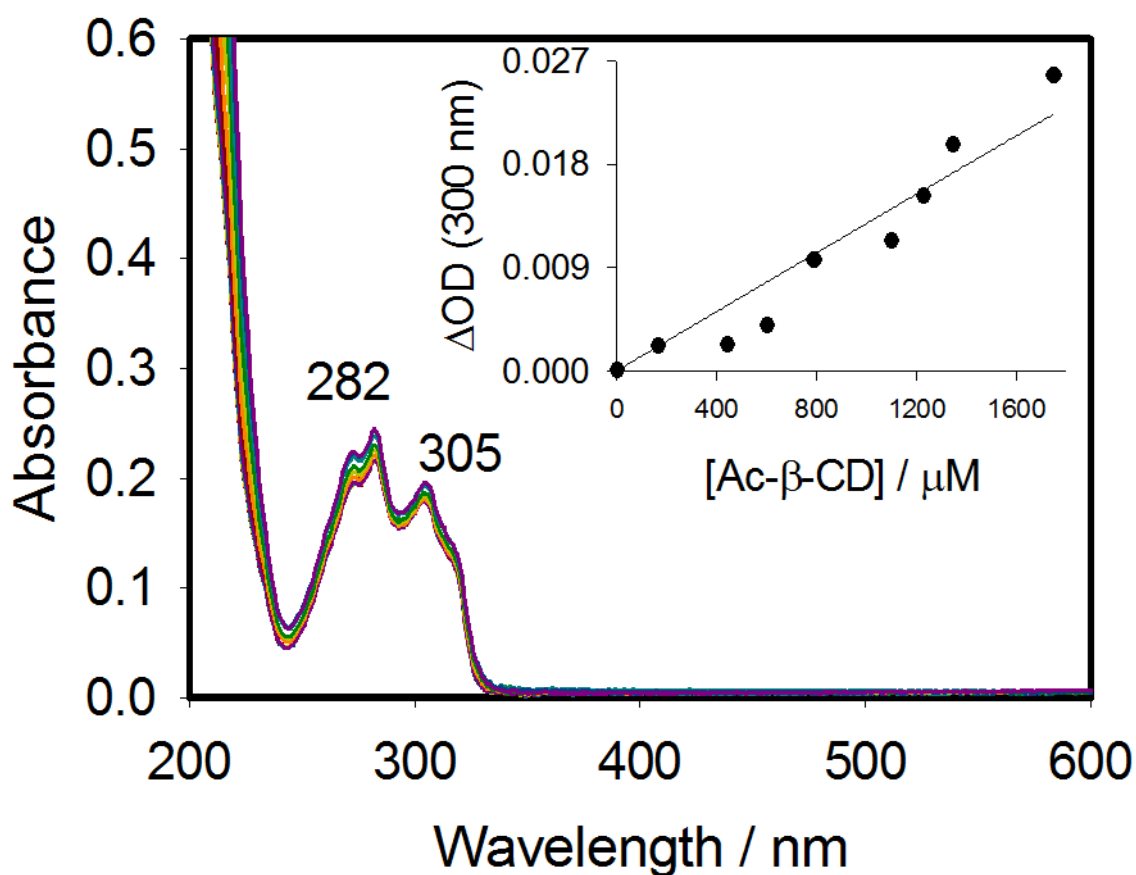


Figure 12 : UV-Visible absorption titration of W (25  $\mu\text{M}$ ) with Ac- $\beta$ -CD at pH 3; the inset shows the corresponding titration curve and the 1:1 binding fit (solid line) with  $K = (5.5 \pm 78) \text{ M}^{-1}$ . The very large error in binding affinity reflects very weak binding

### 3.2.2 Interactions of Warfarin with Ac- $\beta$ -CD at pH 9

In addition to that, even at pH 9 no isosbestic points was noticed as shown in Figure 13. Consequently, Ac- $\beta$ -CD gave no interaction with warfarin at high pH.

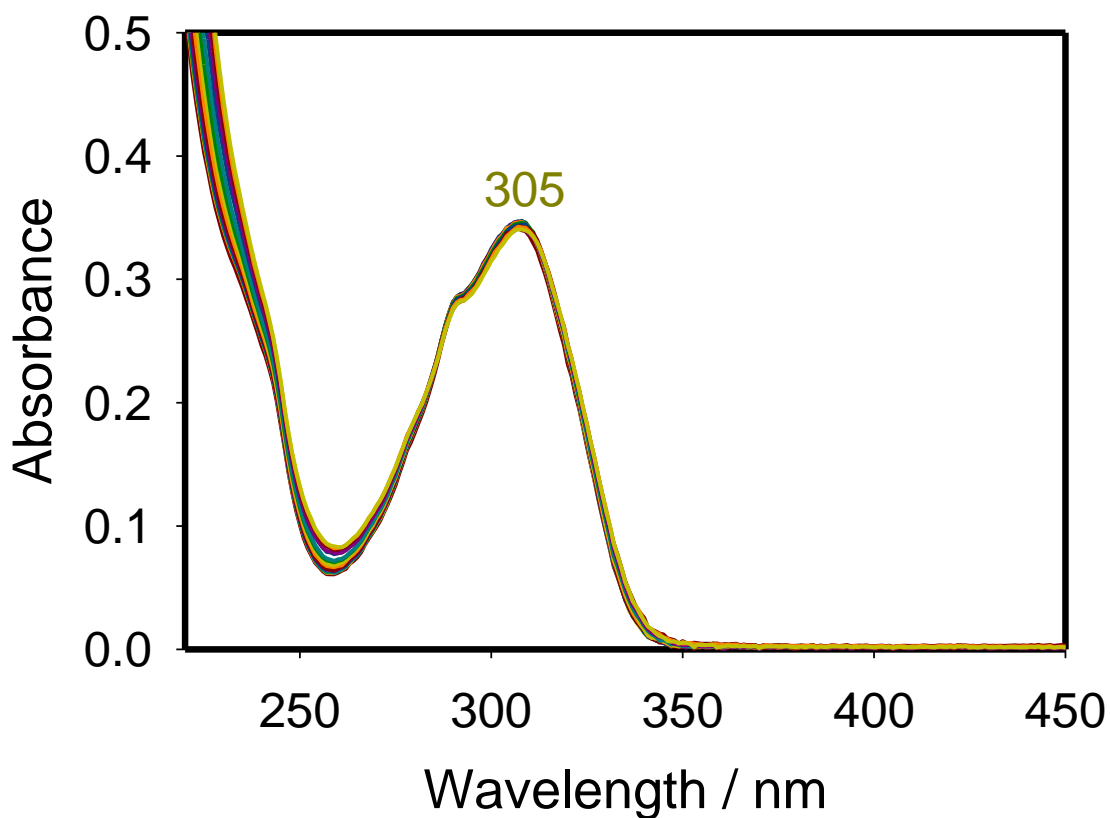


Figure 13: UV-Visible absorption titration of W (25  $\mu$ M) with Ac- $\beta$ -CD at pH 9

### 3.2.3 Interactions of Warfarin with Me- $\beta$ -CD at pH 3

However, previously examined derivative Me- $\beta$ -CD gave the highest binding constants [49]. In Figure 14 at pH 3, only the open protonated form moderately reacts with the host ( $K= 2,900 \text{ M}^{-1}$ ) because isosbestic points were only seen at 305 nm. Vasquez *et al.* indicated that the absorption peak at 310 nm is attributed to the warfarin form with an open side chain, and at 280 nm it is a cyclic hemiketal [46].

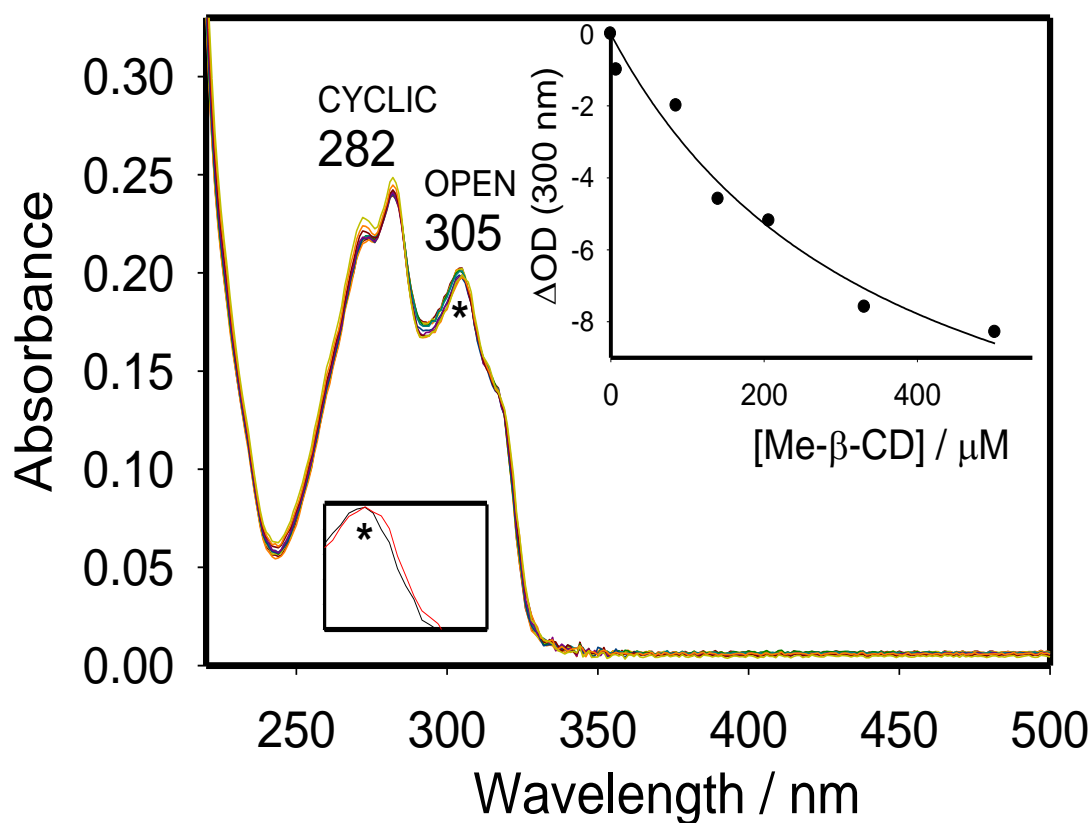


Figure 14: UV–Visible absorption titration of W (25  $\mu\text{M}$ ) with Me- $\beta$ -CD at pH 3; the inset shows the corresponding titration curve and the 1:1 binding fit (solid line) with  $K = (2.9 \pm 0.3) \times 10^3 \text{ M}^{-1}$

### 3.2.4 Interactions of Warfarin with Me- $\beta$ -CD at pH 9

However W- weakly binds CD at high pH (Figure 15) with binding constant of  $420 \text{ M}^{-1}$  in agreement with previous reports [38], [46], [50].

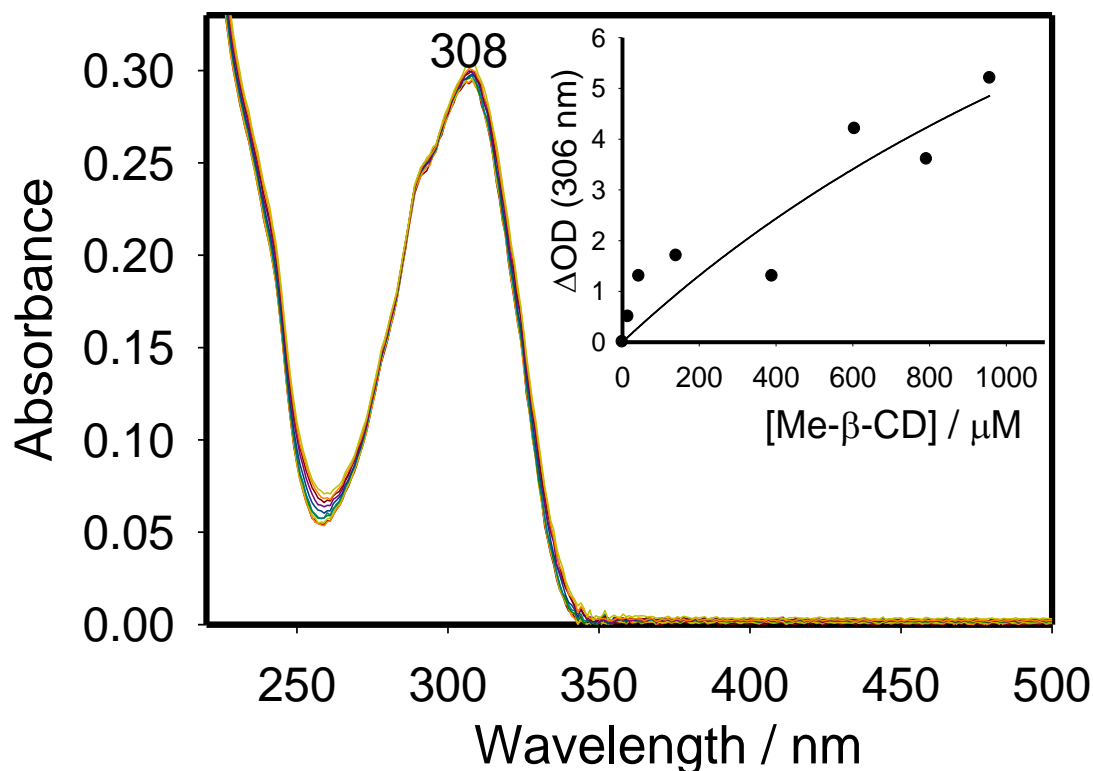


Figure 15: UV–Visible absorption titration of W (25  $\mu\text{M}$ ) with Me- $\beta$ -CD at pH 9; the inset shows the corresponding titration curve and the 1:1 binding fit (solid line) with  $K = (4.2 \pm 1.0) \times 10^2 \text{ M}^{-1}$

Upon addition of Me- $\beta$ -CD host molecules (up to 40 equivalents) to the aqueous solutions of W at pH 3 and 9 (Figure 14,15), characteristic changes in the UV–Visible absorption spectra were observed with the occurrence of several isosbestic points (311 nm, 315 nm, and 320 nm) confirming the formation of a 1:1 binding stoichiometry [46].



The corresponding binding constants between W and Me- $\beta$ -CD at a given pH were derived directly from the optical titration plot at a given wavelength using the formula described in the experimental section.

Absorption spectra upon addition of  $\beta$ -CD to W in water at pH 7.4 (phosphate buffer) were measured by Vullve *et al.*, [46] suggesting that assumption of a 1:1 ratio is valid for this particular molecular complex. W exists predominantly in its open form when bound to  $\beta$ -CD [43], [44]. They attributed this observation to a steric factor that forces W to remain in its open structure. Initially it was expected that hydrophobic cavity of  $\beta$ -CD would stabilize the cyclic form by analogy to earlier report in other hydrophobic media such as Cytochrome P450 2C9 (CYP2C9) [51] .

Addition of  $\beta$ -CD caused less than 10% change in the absorption at 310 nm. These findings support the conclusion made by Vullve *et al.* [46] since only the longest wavelength absorption maxima was affected upon addition of Me- $\beta$ -CD, shifting from 305 nm to 306 nm at pH 3.

### **3.3 Optical Measurements and Host-Induced $pK_a$ Shifts**

A very recent experimental and theoretical investigations by Nowak *et al.* on several hydroxycoumarin derivatives concluded that different location of hydroxyl group should affect the value of  $pK_a$  [52]. Motivated by this work, the changes of absorption spectral profiles of W free and CD-complexes in aqueous solutions was graphed as a function of pH values as shown in Figures 16-19.

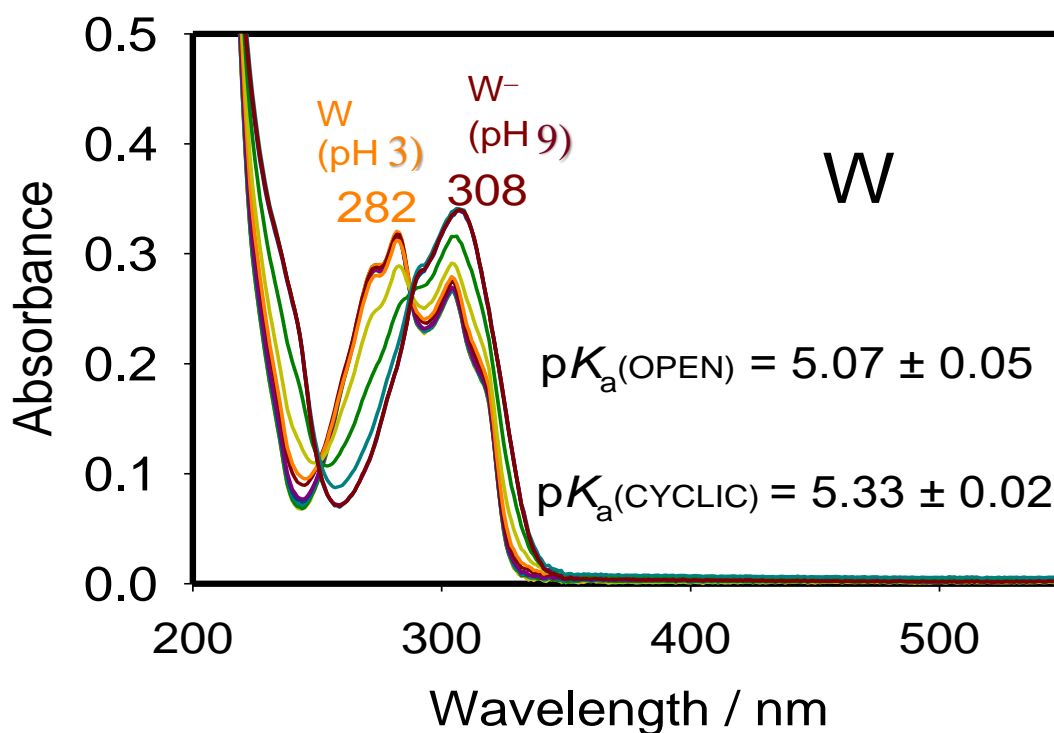


Figure 16: UV-Visible absorption spectra at different pH values of W in water. The sigmoidal fitting error for each extracted pK<sub>a</sub> at 280 (CYCLIC) and 320 nm (OPEN) are shown in the insets

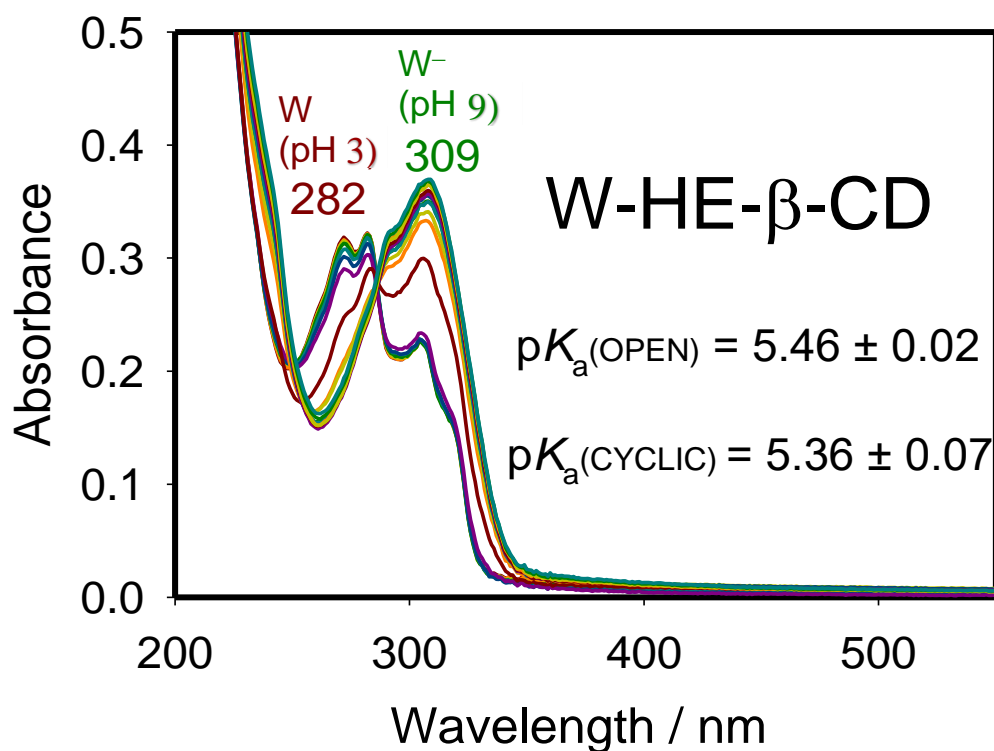


Figure 17: UV-Visible absorption spectra at different pH values of W in HE-β-CD. The sigmoidal fitting error for each extracted pK<sub>a</sub> at 280 (CYCLIC) and 320 nm (OPEN) are shown in the insets

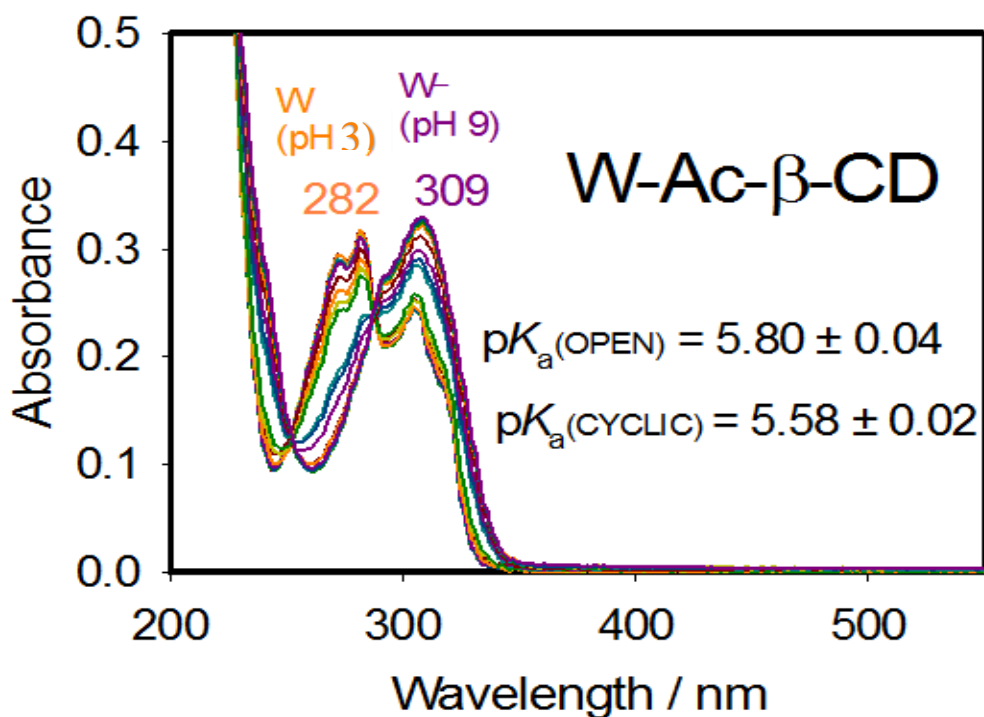


Figure 18: UV-Visible absorption spectra at different pH values of W in Ac- $\beta$ -CD host. The sigmoidal fitting error for each extracted  $pK_a$  at 280 (CYCLIC) and 320 nm (OPEN) are shown in the insets

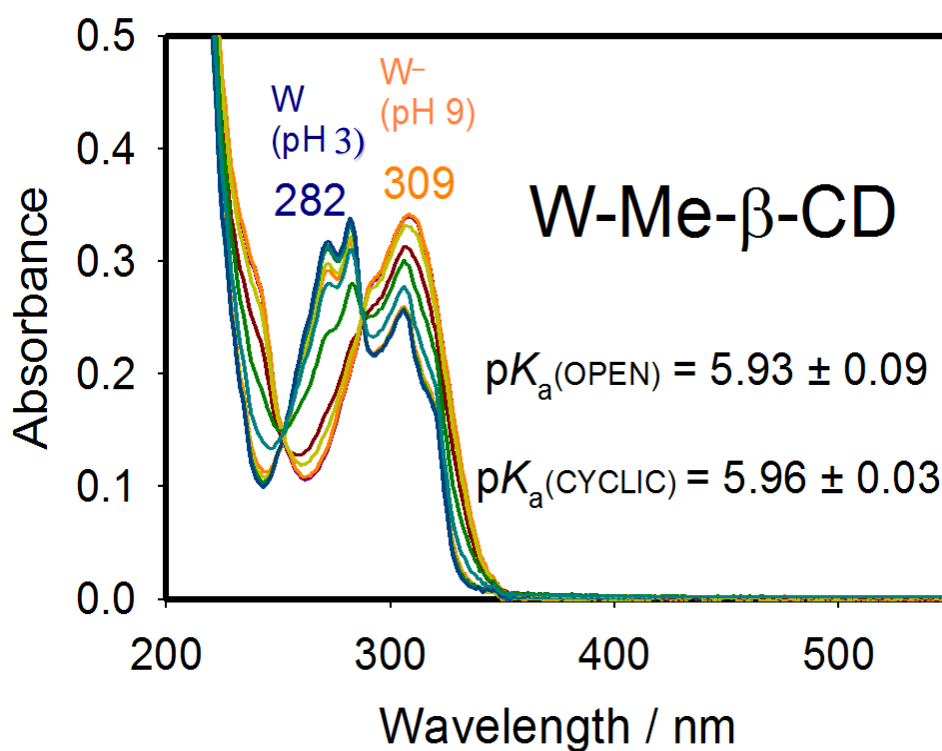


Figure 19: UV-Visible absorption spectra at different pH values of W in ME- $\beta$ -CD. The sigmoidal fitting error for each extracted  $pK_a$  at 280 (CYCLIC) and 320 nm (OPEN) are shown in the insets

Although Me- $\beta$ -CD-induced  $pK_a$  shifts corresponding to the deprotonation processes of the hydroxyl group in coumarin ring (Figure 6) have been studied before by Nowak *et al.* [49], our inspiration specifically comes from the expected dependence of extracted  $pK_a$  values on the selected wavelength in the corresponding titration plots. Also, these experiments should serve fluorescence lifetime data at different pH and confirm the strongest interactions with methylated CDs.

Figures 20-21 illustrated the pH titration plots for the cyclic and open forms. Positive shifts in  $pK_a$  were observed upon addition of all CD derivatives in aqueous solution under similar conditions of ionic strength effects [53]. Regardless of the type of isomer, Me- $\beta$ -CD-assisted  $pK_a$  shifts are always larger than those induced by Ac- $\beta$ -CD ( $\Delta pK_a \sim 0.9$  vs.  $\sim 0.7$  for open forms and  $\sim 0.6$  vs.  $\sim 0.3$  for cyclic forms). The HE- $\beta$ -CD induced the least  $pK_a$  shifts ( $\Delta pK_a \sim 0.4$  for open forms, and no shift observed in case of cyclic forms).

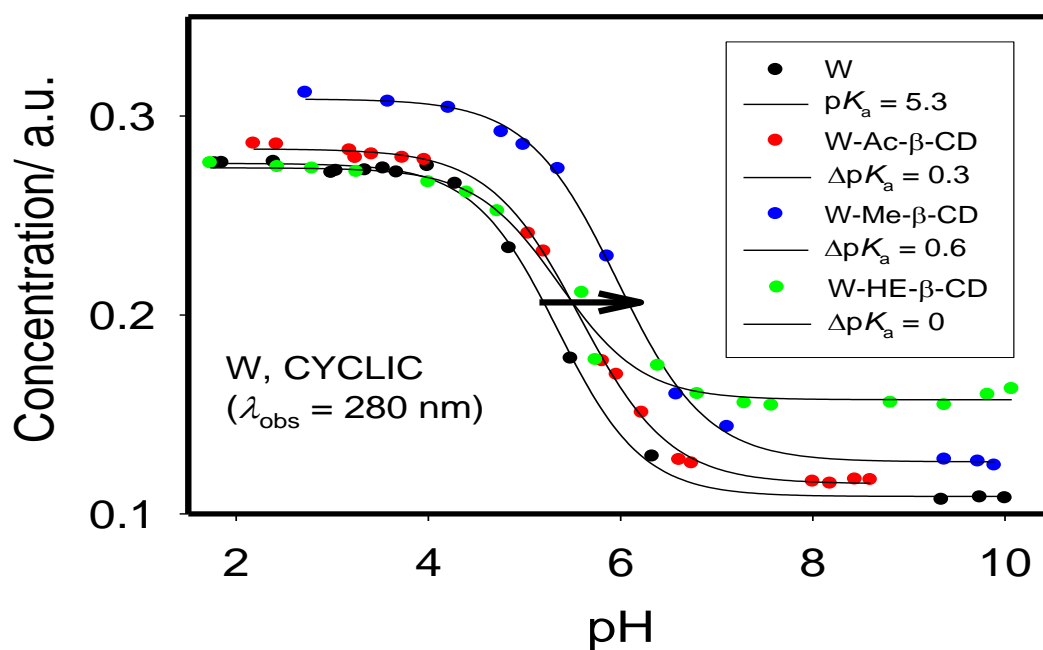


Figure 20: UV-Visible absorption spectra of W in aqueous solutions at different pH values from 2-10 at  $\lambda_{\text{abs}} = 280 \text{ nm}$  in water and inside HE- $\beta$ -CD, Ac- $\beta$ -CD, and Me- $\beta$ -CD. The experimental fitting error for the indicated  $pK_a$  values and the corresponding spectra are shown in Figures 16-19

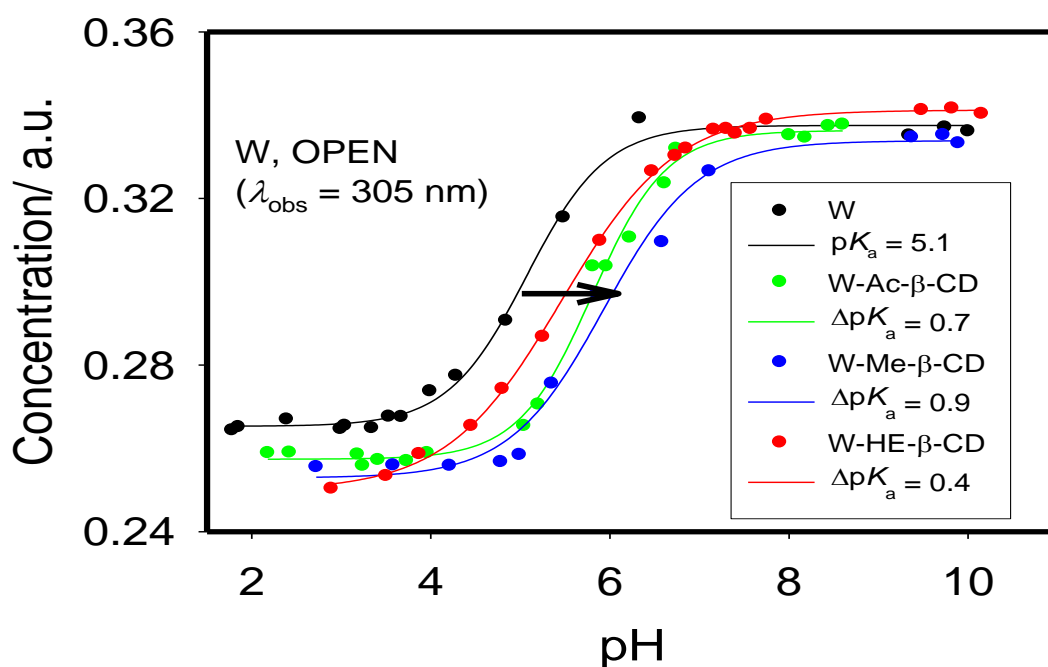


Figure 21: UV-Visible absorption spectra of W in aqueous solutions at different pH values from 2-10  $\lambda_{\text{abs}} = 305$  in water and inside HE- $\beta$ -CD, Ac- $\beta$ -CD, and Me- $\beta$ -CD. The experimental fitting error for the indicated  $pK_a$  values and the corresponding spectra are shown in Figure 16-19

The host-induced  $pK_a$  shifts reflect the changes in the binding affinities of drug to  $\beta$ -CD derivatives in the ground states (see Me- $\beta$ -CD as an example at pH 3 and 9 in Figures 14-15), thus rationalized by the preferential interactions of host towards the protonated form over the deprotonated one [54]. Nowak *et al.*, [49] attributed the strongest  $pK_a$  shifts in Me- $\beta$ -CD to the presence of methyl group that may have preferentially interacted with the CD cavity.

More important to the focus of this work is the observation that upon inclusion in any of the three  $\beta$ -CD hosts, the increase in  $pK_a$  of the open isomer was more pronounced than that of cyclic one, supporting the selective interaction with open form over the cyclic one.

In addition to that, open form of free W appears to be more acidic in ground state ( $pK_a$  5.1 vs. 5.3) than the cyclic one, presumably due to extending electron delocalization in the final charged product ( $W^-$ ) in the former case [52].

### **3.4 Excitation, pH and Cyclodextrin Dependence of Warfarin Steady-State Fluorescence**

This work specifically aimed at investigating the dependence of fluorescence of W on pH and excitation wavelength in the absence and presence of Me- $\beta$ -CD, the host which has sufficiently interacted with W by virtue of the above absorption measurements. Fluorescence pH titration experiment was conducted as illustrated in Figures 22-23. Different  $pK_a$  values were extracted upon exciting W in water at 280 nm and 320 nm ( $pK_a$  6.1 vs. 5.7), which is again attributed to the deprotonation of the hydroxyl proton (Figure 6) with the open form being more acidic.

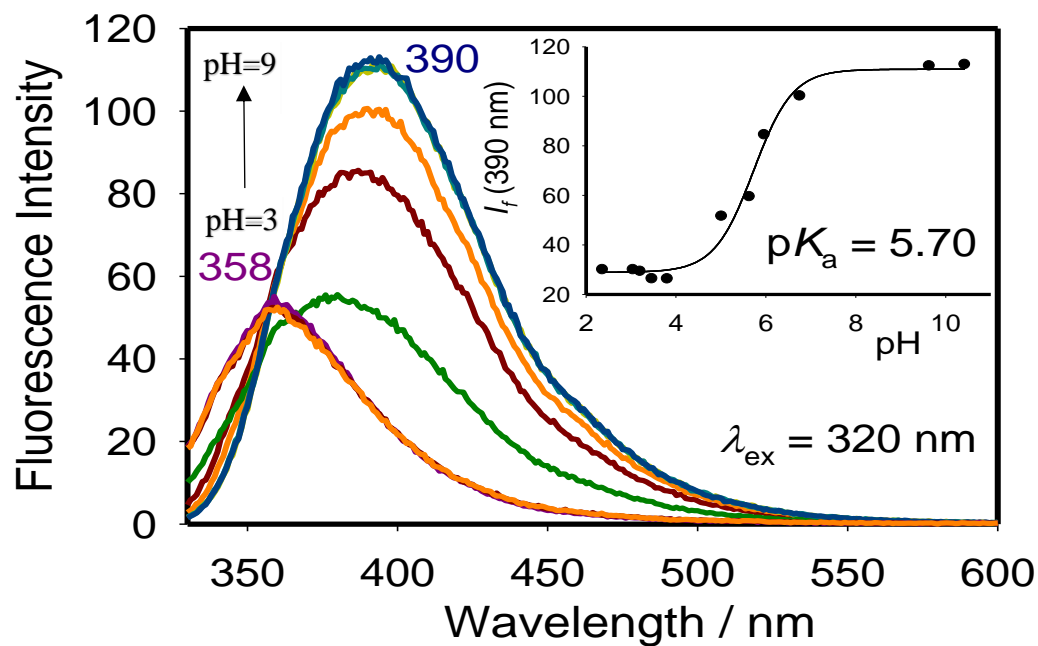


Figure 22: Fluorescence spectra of W (25  $\mu\text{M}$ ) at different pH values with excitation at 320 nm ; the inset shows the experimental fit to a sigmoidal function (solid line), which gives  $\text{p}K_a = 5.70 \pm 0.07$ . Slit widths were 5 nm for excitation and emission

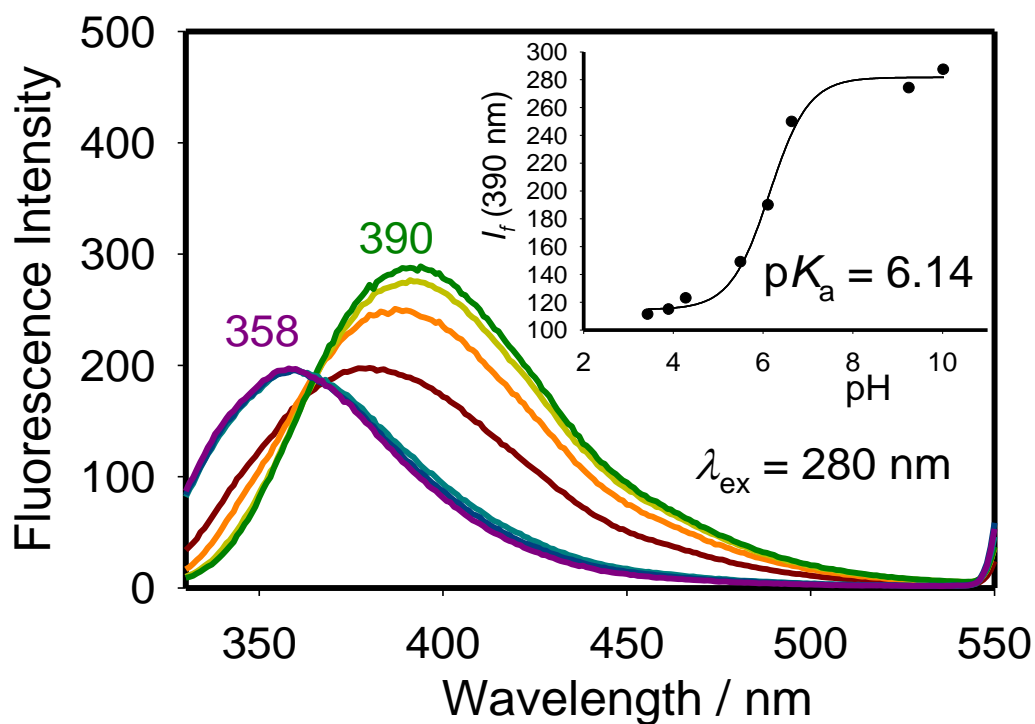


Figure 23: Fluorescence spectra of W (25  $\mu\text{M}$ ) at different pH values with excitation at 280 nm; the inset shows the experimental fit to a sigmoidal function (solid line), which gives  $\text{p}K_a = 6.14 \pm 0.05$ . Slit widths were 5 nm for excitation and 10 nm for emission

This could be ascribed to extended electron delocalization in the excited-state structure of the formed deprotonated form in parallel to the behaviors of isomers in the ground-state [53]. It must be noted that open and cyclic forms, despite having similar emission peaks, gave different emission profile when excited at 280 nm and 320 nm as illustrated in Figure 24, confirming the persistence of intramolecular proton transfer from the open form to cyclic tautomer (Figure 6) in the excited state.

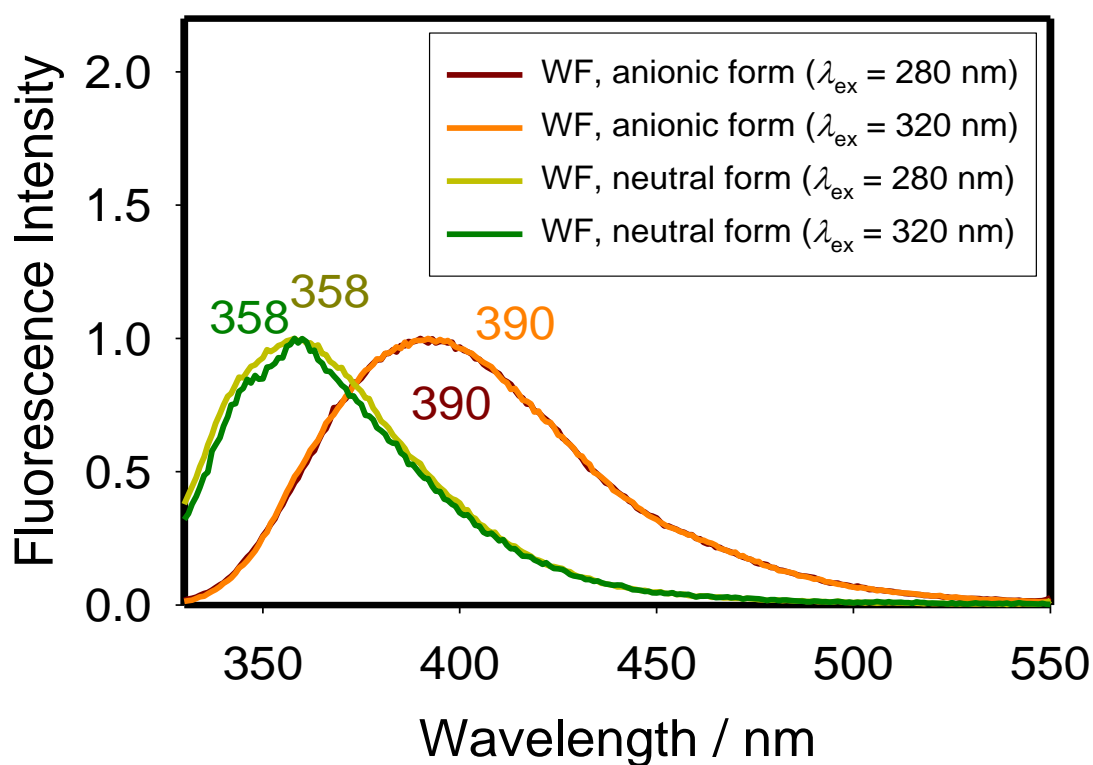


Figure 24: Fluorescence spectra of W (25  $\mu\text{M}$ ) at pH 2.5 and 10 with  $\lambda_{\text{ex}} = 320$  nm and  $\lambda_{\text{ex}} = 280$  nm as labeled by a distinct color. While no change in peak position, spectra of neutral W excited at 280 nm (dark yellow) and 320 nm (dark green) are different



As far as the effects of CDs on emission of W, contrarily to the observed three-fold fluorescence enhancement upon inclusion of W<sup>-</sup> form at pH 9 (Figure 25; excitation at 320 nm) with binding affinity of  $266 \text{ M}^{-1}$  in agreement previous reports [38], [46], [50], the protonated (open or cyclic) forms at pH 3 showed very weak enhancement in fluorescence upon addition of 10 equivalents of host as illustrated in Figures 26-27. These contradictable results warrant further investigations using time-resolved fluorescence spectroscopy.

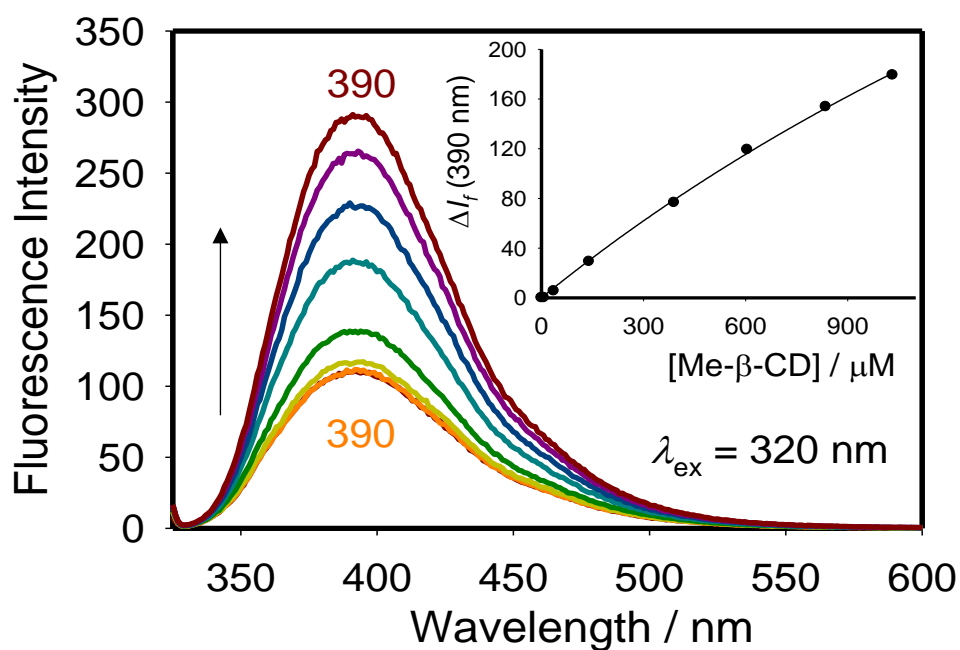


Figure 25: Fluorescence titration of W (25  $\mu\text{M}$ ) with Me- $\beta$ -CD at pH 9 with excitation at 320 nm the inset shows the corresponding titration curve and the 1:1 binding fit (solid line) with  $K = (2.66 \pm 0.06) \times 10^2 \text{ M}^{-1}$

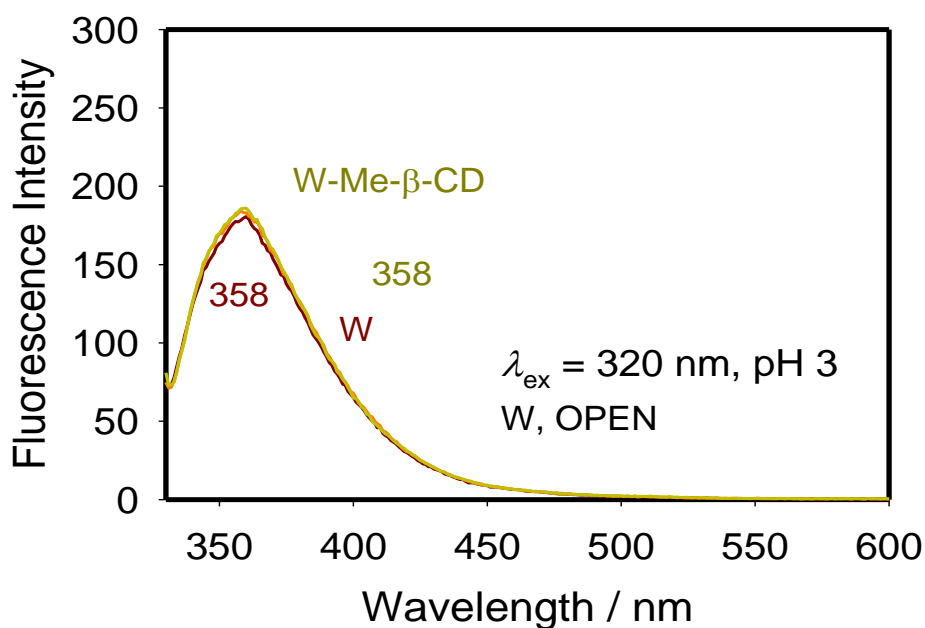


Figure 26: Fluorescence spectra of W (25  $\mu\text{M}$ ) at pH 3 upon the addition of Me- $\beta$ -CD up to 250  $\mu\text{M}$  (10 equiv.) with  $\lambda_{\text{ex}} = 320 \text{ nm}$ , no significant changes in spectra were observed

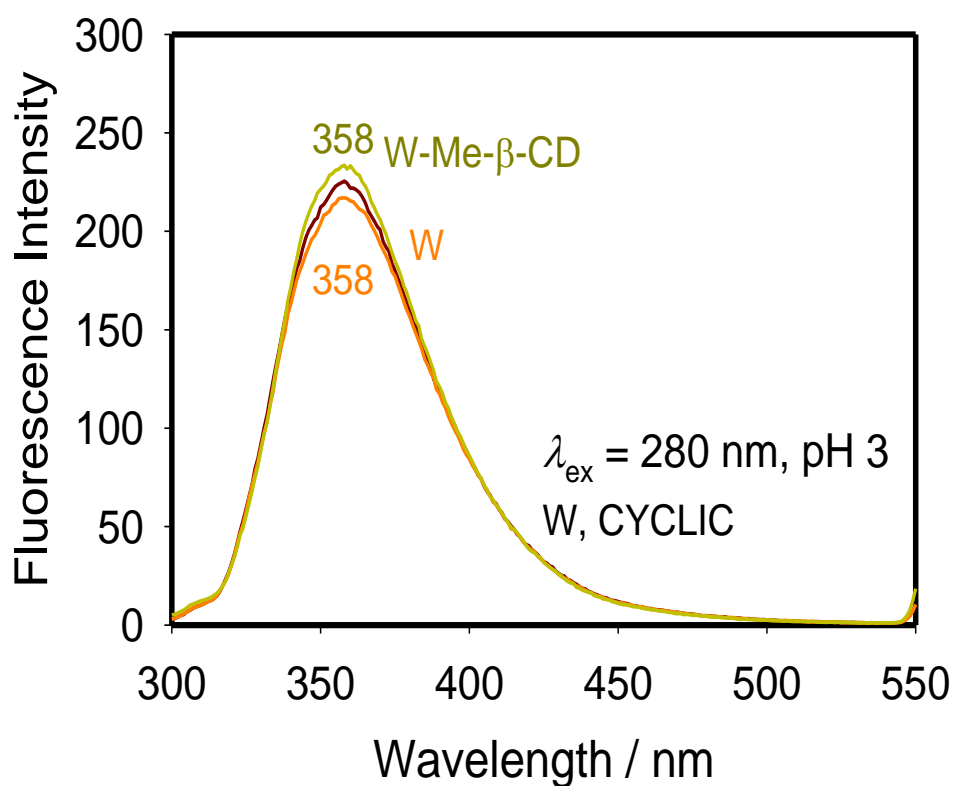


Figure 27: Fluorescence spectra of W (25  $\mu\text{M}$ ) at pH 3 upon the addition of Me- $\beta$ -CD up to 250  $\mu\text{M}$  (10 equiv.) with  $\lambda_{\text{ex}} = 280 \text{ nm}$ , no significant changes in spectra were observed

### 3.5 Fluorescence Lifetime Measurements/Decay-Associated Spectra (DAS)

Time-resolved fluorescence measurements of W at pH 3 and 9 in absence and presence of Me- $\beta$ -CD was opted to rationalize the no enhancement in fluorescence of protonated W upon inclusion compared to those results observed at pH 9. Also sought to separate the sequestering effects of CD on each protonated isomer (open vs. cyclic), by monitoring the change in excited-state lifetime when selectively exciting W at 320 nm and 280 nm, respectively.

Previously, the two forms were simultaneously excited at 300 nm [45]. Emission decays collected every 10 nm across the entire emission spectra of free W at pH 3 upon excitation at 320 nm and 280 were globally fitted to monoexponential decays as shown in Figures 32-33 (Appendix) and tabulated in Table 2.

Table 2: Spectroscopic and photophysical data of W at 25  $\mu$ M in absence and in presence of Me- $\beta$ -CD (1.0 mM). The DAS maximum for each lifetime is given in bracket

Drug Forms	$\lambda_{\text{abs}} / \text{nm}$	$\lambda_{\text{ex}} / \text{nm}$	$\lambda_{\text{em}} / \text{nm}$	$\tau_1 / \text{ns}$ ( $\lambda_{\text{em}} / \text{nm}$ )	$\tau_2 / \text{ns}$ ( $\lambda_{\text{em}} / \text{nm}$ )
W, OPEN (pH 3)	305	320	358	< 0.1	
W, CYCLIC (pH 3)	282	280	358	< 0.2	
W- (pH 9)	308	320	390	< 0.2	
W-Me- $\beta$ -CD, OPEN (pH 3)	306	320 <sup>a</sup>	358	< 0.1 (358)	2.0 $\pm$ 0.4 <sup>b</sup> (375)
W-Me- $\beta$ -CD (pH 9)	309	320	390	< 0.2 (390)	1.22 $\pm$ 0.02 <sup>b</sup> (390)

<sup>a</sup> Upon excitation at 280 nm, no change in excited-state lifetime was observed upon inclusion at pH 3. <sup>b</sup> Values are presented as mean  $\pm$  standard deviation. The estimated experimental error was 20% and 1.6% for the complex lifetimes at pH 3 and 9, respectively.

The excited-state lifetimes appear within our instrument resolution of 90 ps in agreement with others [45]. However, when Me- $\beta$ -CD complex were excited at pH 3 both mono-exponential and biexponential decays were observed as shown in Figures 34-35 (Appendix).

Although addition of CD at pH 3 did not affect the position of peaks (390 nm), excited-state lifetime increased but only when the complex was excited at 320 nm, and not 280 nm (Figure 28, 34 and 35), supporting that Me- $\beta$ -CD host favors the open tautomer form. Even though emission decays of drugs were collected in Figures 28-29 upon addition of 40 equivalents of host (as limited by its solubility in water of about 15 mM), complete formation of complex has not been achieved due to relatively weak binding constant.

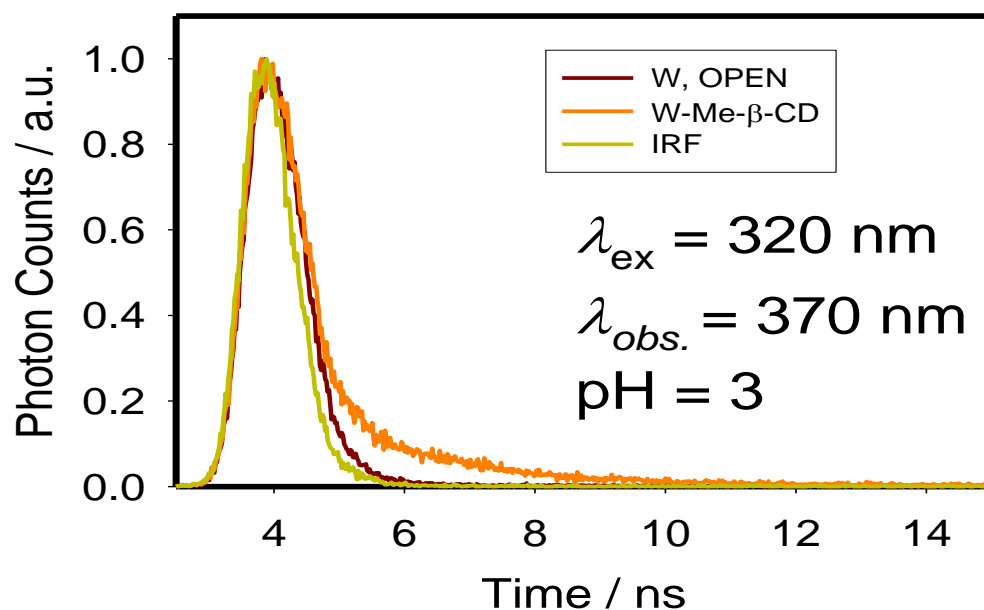


Figure 28: Emission decays collected at 370 nm for W at 25  $\mu\text{M}$  in absence and in presence of Me- $\beta$ -CD (1.0 mM) upon exciting at 320 nm. IRF is the instrument response function of  $\sim 90$  ps

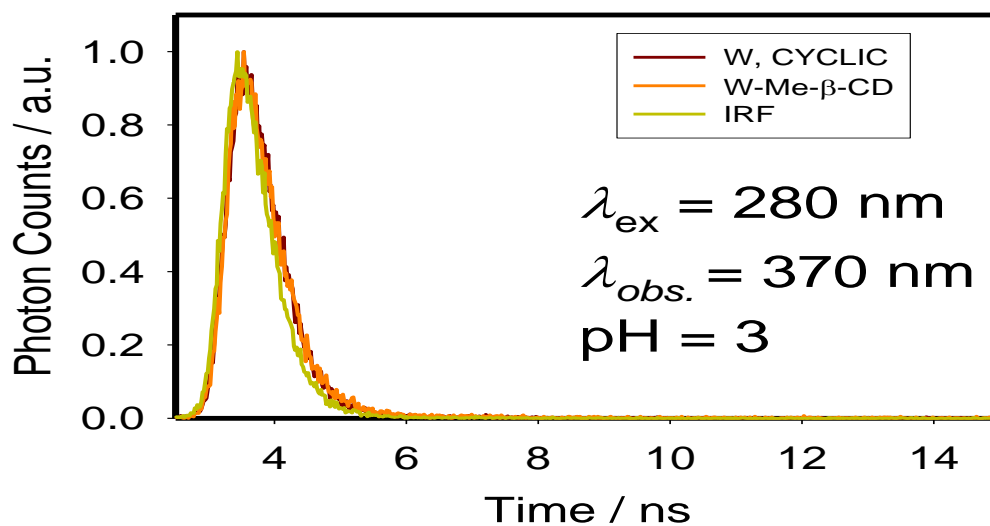


Figure 29: Emission decays collected at 370 nm for W at 25  $\mu\text{M}$  in absence and in presence of Me- $\beta$ -CD (1.0 mM) upon exciting at 280 nm. No change in fluorescence lifetime upon excitation at 280 nm. IRF is the instrument response function of  $\sim 90$  ps

Accordingly, the corresponding DAS spectra in Figures 30-31 (see experimental section) are thus best interpreted by assuming contribution from both free and CD-complexed drug. The emission of free drug at pH 3 dominates the emission spectrum with emission band centered at 358 nm (Figure 30). The corresponding complex at this pH has an emission peak at  $\sim 375$  nm with a longer excited-state lifetime  $\sim 2.0$  ns, yet a much lower emission quantum yield (0.006 vs. 0.0005 in Table 3).

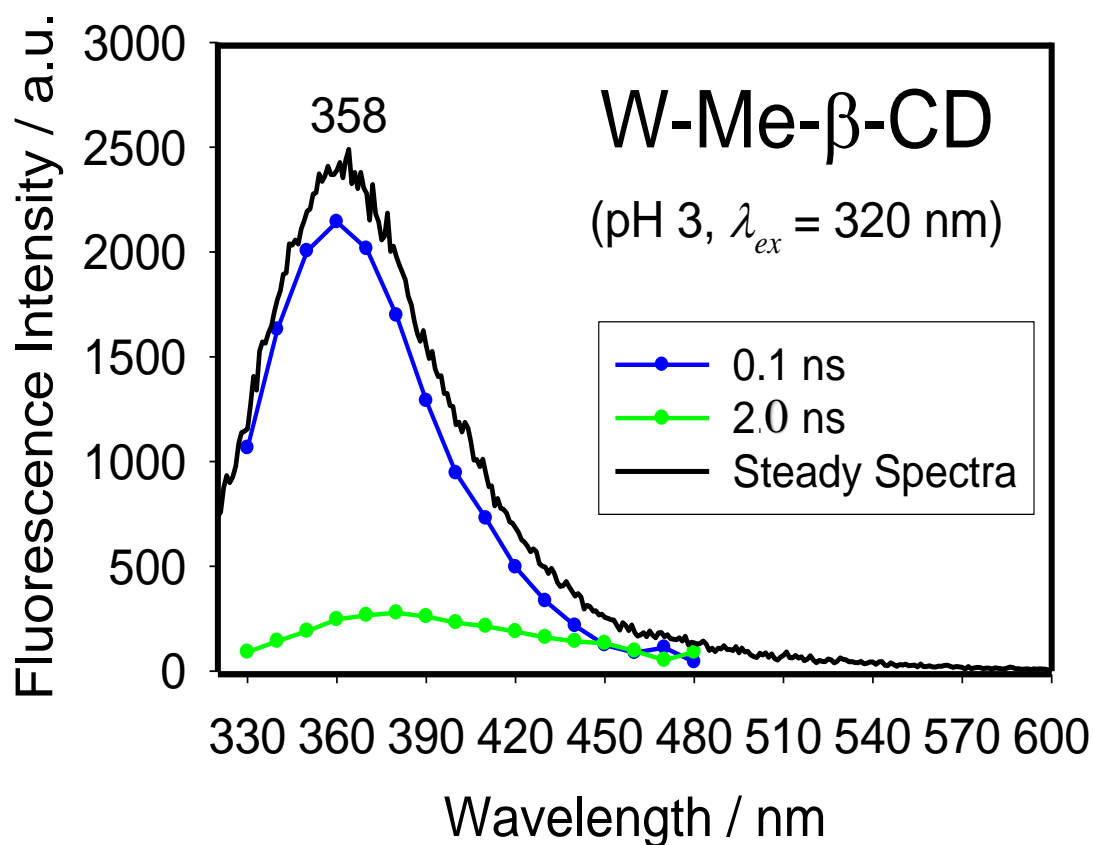


Figure 30: Decay-associated spectra (DAS) of two-component mixture of fluorphores for W-Me-β-CD host-guest complex (25  $\mu$ M for W and 1 mM for W-Me-β-CD) at pH 3 upon exciting at 320 nm at room temperature. The corresponding steady-state spectra of each solution are also shown for comparison (see experimental section)

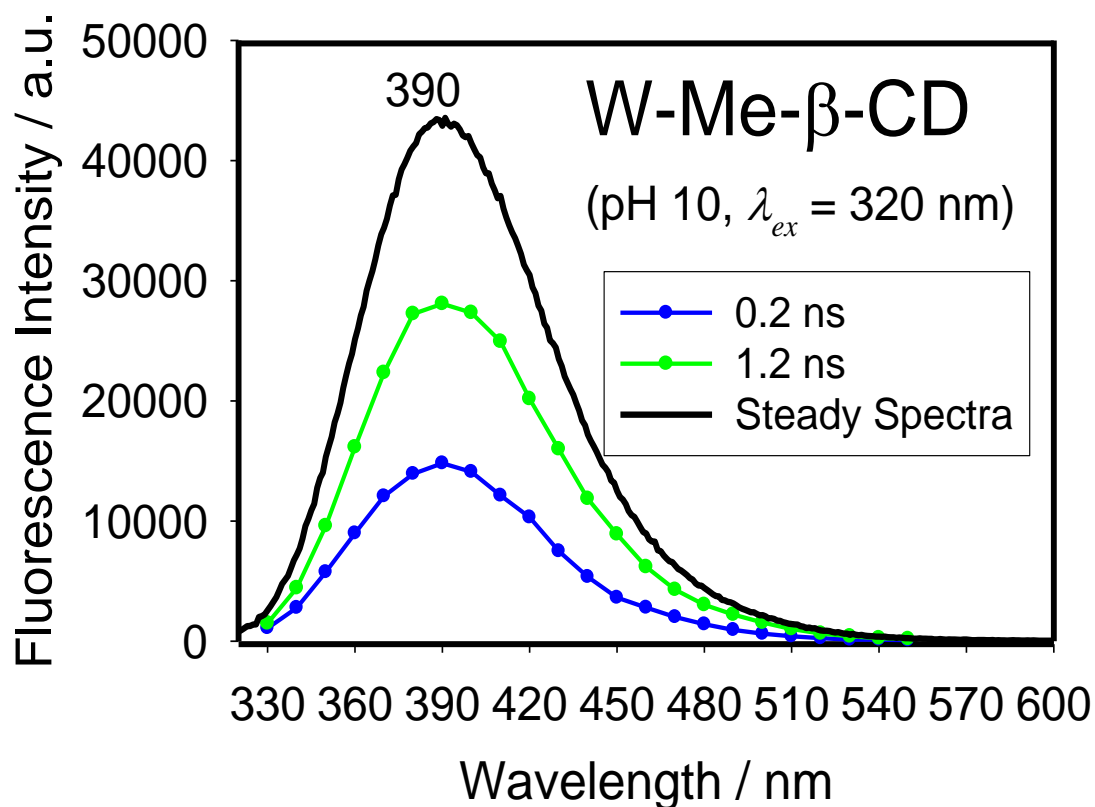


Figure 31: Decay-associated spectra (DAS) of two-component mixture of fluorphores for W-Me-β-CD host-guest complex (25 μM for W and 1 mM for W-Me-β-CD) at pH 10 and upon exciting at 320 nm at room temperature. The corresponding steady-state spectra of each solution are also shown for comparison (see experimental section)

Separation of the two lifetimes by DAS method enables us to calculate radiative ( $k_r$ ) and non-radiative rate constants ( $k_{nr}$ ) alongside emission quantum yield ( $\Phi_F$ ) upon complexation of W to Me-β-CD, as illustrated in Table 3.

Table 3: Fluorescence quantum yield  $\Phi_F$ , Radiative rate constant  $k_r$ , and Non-radiative rate constant  $k_{nr}$

Drug Forms	$\lambda_{ex}$ / nm	$\Phi_F (\times 10^{-3})^a$	$k_r (\times 10^7 \text{ s}^{-1})^b$	$k_{nr} (\times 10^9 \text{ s}^{-1})^b$	$\tau$ / ns (Mean)
W OPEN	320	$6 \pm 0.01$	$> 6$	$> 10$	$< 0.1$
W-	320	$12 \pm 0.01$	$> 12$	$> 10$	$< 0.1$
Me- $\beta$ -CD OPEN	320	$0.5 \pm 0.01$	0.02	0.50	2.0
W-Me- $\beta$ -CD	320	$24 \pm 0.01$	2.0	0.81	1.22

<sup>a</sup>Measured using warfarin (W) in phosphate-buffered saline (PBS, pH ~7.4, 10 mM sodium phosphate) as the standard ( $\Phi_F = 0.012$ ) [46], and calculated using the known equation [55]:  $\Phi_{unk} = \Phi_{std} \left( \frac{I_{unk}}{A_{unk}} \right) \left( \frac{A_{std}}{I_{std}} \right) \left( \frac{n_{unk}}{n_{std}} \right)^2$ , where n is the refractive indices for the standard (std) and experimental (unk) solvents, I is the fluorescence integral of the emission between 300 and 550 nm, and A is the absorbance at the excitation wavelength. <sup>b</sup> Calculated using the known equations:  $\Phi = \frac{k_r}{k_r + k_{nr}}$ ,  $\tau = \frac{1}{k_r + k_{nr}}$ ,  $k_{nr} = \frac{1 - \Phi}{\tau}$ , and  $k_r = \frac{\Phi}{\tau}$ .

The variations of  $k_r$  values in the absence and presence of CD are difficult to explain because of the unreliable measurement of lifetimes in water. However, the red shifts of emission peaks of W upon complexation to Me- $\beta$ -CD hosts at pH 3 despite their non-polar hydrophobic and rigid cavity along with concomitant significant decrease of the  $k_r$  values by ~2 orders of magnitude, from  $k_r = \sim 6 \times 10^7$  to  $2 \times 10^5 \text{ s}^{-1}$ , means that the enhancement in excited-state lifetimes is best described by a radiative-rate law [55].

This argument is supported by the boarder UV-visible spectrum of W when compared to that spectrum in water upon inclusion to CD, as shown in Figure 14 and in light of Strickler-Berg equation [55]. Karlsson et al. [45] pointed out the possibility of attributing the longer lifetime of W observed in ethanol (0.45 ns,  $\lambda_{ex} = 295 \text{ nm}$ ) to the formation of solute-solvent hydrogen-bonded complexes.



Dondon et al. [56] also posited that for other 4-hydroxycoumarin derivatives similar hydrogen-bonded complexes could have formed between the coumarin lactone group and the CD secondary hydroxyl groups. It transpires that there is a plausible explanation to the fluorescence behaviors of protonated W-CD systems that similar hydrogen-bonded complexes have formed between CD secondary hydroxyl group and the carbonyl group of open form, which the cyclic form lacks.

It is worth to mention that the low binding affinity of our W-CD system in the present study limits its potential use for biomedical applications as a large fraction of free guest will always persist at any concentration of the added host.

However, understanding the factors that enhance the binding constants of W with CDs such as the formation of hydrogen bonded complexes [45], [56] and the presence of methyl groups [49] alongside the investigation of pH effects on the complex stability should preclude further studies in the future on W-CD systems for the establishment of pH-driven stimuli-responsive systems.

Emission decays collected at pH 9 Figure 36 and 37 (Appendix) gave DAS spectra (Figure 31) that demonstrated opposite effects induced by CD addition. In agreement with previous reports [46], [51], [57], the complex at pH 9 excited at 320 nm has a higher emission yields than that of free drug with excited-state lifetime of 1.22 ns and no change in peak position at ~ 390 nm (Table 3). Vasquez *et al.*, suggested encapsulation of deprotonated W forms considerably suppresses the vibronic modes that provide pathways for non-radiative transitions between the excited and ground states of W, causing a decrease in the rates of the non-radiative decay processes.

Indeed, calculation supports these findings and the operation of energy-gap law in which the excited state  $S_1$  is more polar than the ground state  $S_0$ . Consequently,  $S_1$  state will be much more destabilized in a nonpolar medium than the  $S_0$  state. Such an increase in energy gap results in a decrease in  $k_{nr}$  [58].

While non-radiate rate constants in Table 3 decreases  $\sim 12$  times upon inclusion in the hydrophobic interior of Me- $\beta$ -CD, radiative rate constants decreases only  $\sim 6$  times. The increase in lifetimes and associated decrease in  $k_{nr}$  of other 4-hydroxycoumarin derivatives [56] from below 0.5 ns to 1.1–1.3 ns (depending on the derivative) was also observed upon sequestration of dyes into  $\beta$ -CD macromolecules.

## Chapter 4: Conclusion

In this work, time-resolved fluorescence spectra measured using picoseconds laser diode at 280 nm and 320 nm with selective exciting of isomers of W were conducted utilizing both global and target analysis to give more specific information about nature and dynamics of excited-states of warfarin in water and inside cyclodextrins. An increase in excited-state lifetime of warfarin was observed upon its interaction with Me- $\beta$ -CD with selective interactions towards the open form. The increase in lifetime of open form was explained by radiative rate law, while that of deprotonated form by energy-gap law. Lower acidity of the open form have been demonstrated.

Fluorescence properties of W inside cyclodextrins in aqueous solutions have attracted attentions in several occasions due to their implications in bioanalytical quantification of W in commercial pesticides [50], [59]–[61] or biological liquids [62] and in utilizing W as fluorescent probes or site marker to study drug-protein interactions [63], [64].

In addition to fluorescence properties better understanding of the interactions of W with cyclodextrin in ground-state should lead to better control on modulating its  $pK_a$  values in solution [38], [49], with implications in analytical separation of drug by electrophoresis [53] liquid chromatography [65], [66], as well as its formulations [67] or clinical studies [68].

In summary, these results give the structures present in cyclodextrin environment in ground-state and explain their kinetic behaviors in excited-state using quantitative time-resolved fluorescence tools, collectively leading to better

understanding on the role of cyclodextrin on manipulating the function of this anticoagulant drug in ground and excited states.

#### **4.1 Recommendations**

The following recommendations are suggested as possible ways to extend this study:

1- Study the host-guest interactions of W with different macromolecules such as cucurbit[n]uril and other different cyclodextrins.

2- Warfarin was selected because it is commercially used as drug that favors blood bleeding, while finding a stimuli (chemical competitor) that tune the form (open and cyclic) could control blood clotting/bleeding balance in the future.

3- Study the photochemistry of other drugs and the encapsulation of these drugs with different macromolecules.

## References

- [1] J.-M. Lehn, "Supramolecular chemistry—scope and perspectives molecules, supermolecules, and molecular devices (Nobel Lecture)," *Angew. Chem. Int. Ed. Engl.*, vol. 27, no. 1, pp. 89–112, 1988.
- [2] N. Saleh, I. Ghosh, and W. M. Nau, "Cucurbiturils in drug delivery and for biomedical applications," in *Supramolecular systems in biomedical fields*, RSC Publishing: Cambridge, UK, 2013, pp. 164–212.
- [3] X. Ma and Y. Zhao, "Biomedical applications of supramolecular systems based on host–guest interactions," *Chem. Rev.*, vol. 115, no. 15, pp. 7794–7839, 2014.
- [4] J. W. Steed and J. L. Atwood, *Supramolecular chemistry*, 2nd ed. Chichester, UK: Wiley, 2009.
- [5] L. Isaacs, "Stimuli responsive systems constructed using cucurbit [n] uril-type molecular containers," *Acc. Chem. Res.*, vol. 47, no. 7, pp. 2052–2062, 2014.
- [6] B. Rybtchinski, "Adaptive supramolecular nanomaterials based on strong noncovalent interactions," *Acs Nano*, vol. 5, no. 9, pp. 6791–6818, 2011.
- [7] V. J. Stella and R. A. Rajewski, "Cyclodextrins: their future in drug formulation and delivery," *Pharm. Res.*, vol. 14, no. 5, pp. 556–567, 1997.
- [8] V. D. Uzunova, C. Cullinane, K. Brix, W. M. Nau, and A. I. Day, "Toxicity of cucurbit [7] uril and cucurbit [8] uril: an exploratory in vitro and in vivo study," *Org. Biomol. Chem.*, vol. 8, no. 9, pp. 2037–2042, 2010.
- [9] J. M. Zayed, N. Nouvel, U. Rauwald, and O. A. Scherman, "Chemical complexity—supramolecular self-assembly of synthetic and biological building blocks in water," *Chem. Soc. Rev.*, vol. 39, no. 8, pp. 2806–2816, 2010.
- [10] Y. Zhao *et al.*, "Progressive Macromolecular Self-Assembly: From Biomimetic Chemistry to Bio-Inspired Materials," *Adv. Mater.*, vol. 25, no. 37, pp. 5215–5256, 2013.
- [11] X. Yan, F. Wang, B. Zheng, and F. Huang, "Stimuli-responsive supramolecular polymeric materials," *Chem. Soc. Rev.*, vol. 41, no. 18, pp. 6042–6065, 2012.
- [12] T. Loftsson and D. Duchêne, "Cyclodextrins and their pharmaceutical applications," *Int. J. Pharm.*, vol. 329, no. 1–2, pp. 1–11, 2007.

- [13] E. Masson, X. Ling, R. Joseph, L. Kyeremeh-Mensah, and X. Lu, "Cucurbituril chemistry: a tale of supramolecular success," *RSC Adv.*, vol. 2, no. 4, pp. 1213–1247, Jan. 2012.
- [14] M. V. Rekharsky and Y. Inoue, "Complexation thermodynamics of cyclodextrins," *Chem. Rev.*, vol. 98, no. 5, pp. 1875–1918, 1998.
- [15] T. Irie and K. Uekama, "Cyclodextrins in peptide and protein delivery," *Adv. Drug Deliv. Rev.*, vol. 36, no. 1, pp. 101–123, 1999.
- [16] S. Moghaddam *et al.*, "New ultrahigh affinity host-guest complexes of cucurbit [7] uril with bicyclo [2.2. 2] octane and adamantane guests: Thermodynamic analysis and evaluation of m2 affinity calculations," *J. Am. Chem. Soc.*, vol. 133, no. 10, pp. 3570–3581, 2011.
- [17] N. Saleh, A. L. Koner, and W. M. Nau, "Activation and Stabilization of Drugs by Supramolecular pKa Shifts: Drug-Delivery Applications Tailored for Cucurbiturils," *Angew. Chem.*, vol. 120, no. 29, pp. 5478–5481, 2008.
- [18] J. Kim *et al.*, "New cucurbituril homologues: syntheses, isolation, characterization, and X-ray crystal structures of cucurbit [n] uril (n= 5, 7, and 8)," *J. Am. Chem. Soc.*, vol. 122, no. 3, pp. 540–541, 2000.
- [19] A. Day, A. P. Arnold, R. J. Blanch, and B. Snushall, "Controlling factors in the synthesis of cucurbituril and its homologues," *J. Org. Chem.*, vol. 66, no. 24, pp. 8094–8100, 2001.
- [20] J. W. Lee, S. Samal, N. Selvapalam, H.-J. Kim, and K. Kim, "Cucurbituril homologues and derivatives: new opportunities in supramolecular chemistry," *Acc. Chem. Res.*, vol. 36, no. 8, pp. 621–630, 2003.
- [21] Q. Li *et al.*, "Encapsulation of alkyldiammonium ions within two different cavities of twisted cucurbit [14] uril," *Chem. Commun.*, vol. 52, no. 12, pp. 2589–2592, 2016.
- [22] M. Shaikh, J. Mohanty, P. K. Singh, W. M. Nau, and H. Pal, "Complexation of acridine orange by cucurbit [7] uril and  $\beta$ -cyclodextrin: photophysical effects and p K a shifts," *Photochem. Photobiol. Sci.*, vol. 7, no. 4, pp. 408–414, 2008.
- [23] J. Mohanty, A. C. Bhasikuttan, W. M. Nau, and H. Pal, "Host- Guest Complexation of Neutral Red with Macrocyclic Host Molecules: Contrasting p K a Shifts and Binding Affinities for Cucurbit [7] uril and  $\beta$ -Cyclodextrin," *J. Phys. Chem. B*, vol. 110, no. 10, pp. 5132–5138, 2006.
- [24] X. Zhang, G. Gramlich, X. Wang, and W. M. Nau, "A Joint Structural, Kinetic, and Thermodynamic Investigation of Substituent Effects on Host- Guest

Complexation of Bicyclic Azoalkanes by  $\beta$ -Cyclodextrin," *J. Am. Chem. Soc.*, vol. 124, no. 2, pp. 254–263, 2002.

[25] V. Sindelar, S. Silvi, and A. E. Kaifer, "Switching a molecular shuttle on and off: simple, pH-controlled pseudorotaxanes based on cucurbit [7] uril," *Chem. Commun.*, vol. 0, no. 20, pp. 2185–2187, 2006.

[26] N. Saleh, A. L. Koner, and W. M. Nau, "Activation and Stabilization of Drugs by Supramolecular pKa Shifts: Drug-Delivery Applications Tailored for Cucurbiturils," *Angew. Chem.*, vol. 120, no. 29, pp. 5478–5481, 2008.

[27] C. Marquez and W. M. Nau, "Two Mechanisms of Slow Host–Guest Complexation between Cucurbit [6] uril and Cyclohexylmethylamine: pH-Responsive Supramolecular Kinetics," *Angew. Chem. Int. Ed.*, vol. 40, no. 17, pp. 3155–3160, 2001.

[28] A. D. St-Jacques, I. W. Wyman, and D. H. Macartney, "Encapsulation of charge-diffuse peralkylated onium cations in the cavity of cucurbit [7] uril," *Chem. Commun.*, vol. 0, no. 40, pp. 4936–4938, 2008.

[29] I. W. Wyman and D. H. Macartney, "Cucurbit [7] uril host–guest complexes of cholines and phosphonium cholines in aqueous solution," *Org. Biomol. Chem.*, vol. 8, no. 1, pp. 253–260, 2010.

[30] M. Shaikh, J. Mohanty, P. K. Singh, W. M. Nau, and H. Pal, "Complexation of acridine orange by cucurbit [7] uril and  $\beta$ -cyclodextrin: photophysical effects and p K a shifts," *Photochem. Photobiol. Sci.*, vol. 7, no. 4, pp. 408–414, 2008.

[31] A. L. Koner and W. M. Nau, "Cucurbituril encapsulation of fluorescent dyes," *Supramol. Chem.*, vol. 19, no. 1–2, pp. 55–66, 2007.

[32] A. L. Koner, I. Ghosh, N. Saleh, and W. M. Nau, "Supramolecular encapsulation of benzimidazole-derived drugs by cucurbit [7] uril," *Can. J. Chem.*, vol. 89, no. 2, pp. 139–147, 2011.

[33] M. Danaher, H. De Ruyck, S. R. Crooks, G. Dowling, and M. O’Keeffe, "Review of methodology for the determination of benzimidazole residues in biological matrices," *J. Chromatogr. B*, vol. 845, no. 1, pp. 1–37, 2007.

[34] B. Tang, X. Wang, H. Liang, B. Jia, and Z. Chen, "Study on the supramolecular interaction of thiabendazole and  $\beta$ -cyclodextrin by spectrophotometry and its analytical application," *J. Agric. Food Chem.*, vol. 53, no. 22, pp. 8452–8459, 2005.

- [35] N. Saleh, M. A. Meetani, L. Al-Kaabi, I. Ghosh, and W. M. Nau, "Effect of cucurbit [n] urils on tropicamide and potential application in ocular drug delivery," *Supramol. Chem.*, vol. 23, no. 9, pp. 650–656, 2011.
- [36] P. N. Patil, "Some factors which affect the ocular drug responses," *Trends Pharmacol. Sci.*, vol. 5, pp. 201–204, 1984.
- [37] K. Pal, F. Chandra, S. Mallick, and A. L. Koner, "Effect of solvents and cyclodextrin complexation on acid–base and photophysical properties of dapoxyl dye," *J. Photochem. Photobiol. Chem.*, vol. 306, pp. 47–54, 2015.
- [38] S. Datta and M. Halder, "Effect of encapsulation in the anion receptor pocket of sub-domain IIA of human serum albumin on the modulation of pKa of warfarin and structurally similar acidic guests: A possible implication on biological activity," *J. Photochem. Photobiol. B*, vol. 130, pp. 76–85, 2014.
- [39] R. Wallin and S. M. Hutson, "Warfarin and the vitamin K-dependent  $\gamma$ -carboxylation system," *Trends Mol. Med.*, vol. 10, no. 7, pp. 299–302, 2004.
- [40] L. L. Woods and S. M. Shamma, "Synthesis of substituted coumarins with fluorescent properties," *J. Chem. Eng. Data*, vol. 16, no. 1, pp. 101–102, 1971.
- [41] B. D. Wagner, "The use of coumarins as environmentally-sensitive fluorescent probes of heterogeneous inclusion systems," *Molecules*, vol. 14, no. 1, pp. 210–237, 2009.
- [42] N. Saleh, Y. A. Al-Soud, L. Al-Kaabi, I. Ghosh, and W. M. Nau, "A coumarin-based fluorescent PET sensor utilizing supramolecular pKa shifts," *Tetrahedron Lett.*, vol. 52, no. 41, pp. 5249–5254, 2011.
- [43] E. J. Valente, E. C. Lingafelter, W. R. Porter, and W. F. Trager, "Structure of warfarin in solution," *J. Med. Chem.*, vol. 20, no. 11, pp. 1489–1493, 1977.
- [44] E. J. Valente and W. F. Trager, "Anomalous chiroptical properties of warfarin and phenprocoumon," *J. Med. Chem.*, vol. 21, no. 1, pp. 141–143, 1978.
- [45] B. C. Karlsson, A. M. Rosengren, P. O. Andersson, and I. A. Nicholls, "The spectrophysics of warfarin: Implications for protein binding," *J. Phys. Chem. B*, vol. 111, no. 35, pp. 10520–10528, 2007.
- [46] J. M. Vasquez, A. Vu, J. S. Schultz, and V. I. Vullev, "Fluorescence enhancement of warfarin induced by interaction with  $\beta$ -cyclodextrin," *Biotechnol. Prog.*, vol. 25, no. 4, pp. 906–914, 2009.
- [47] D. P. Millar, "Time-resolved fluorescence spectroscopy," *Curr. Opin. Struct. Biol.*, vol. 6, no. 5, pp. 637–642, 1996.



- [48] E. P. Farr, J. C. Quintana, V. Reynoso, J. D. Ruberry, W. R. Shin, and K. R. Swartz, "Introduction to Time-Resolved Spectroscopy: Nanosecond Transient Absorption and Time-Resolved Fluorescence of Eosin B," *J. Chem. Educ.*, vol. 95, no. 5, pp. 864–871, 2018.
- [49] P. M. Nowak, M. Woźniakiewicz, M. P. Mitoraj, M. Garnysz, and P. Kościelniak, "Modulation of pKa by cyclodextrins; subtle structural changes induce spectacularly different behaviors," *RSC Adv.*, vol. 5, no. 95, pp. 77545–77552, Sep. 2015.
- [50] S. Ishiwata and M. Kamiya, "Cyclodextrin inclusion effects on fluorescence and fluorimetric properties of the pesticide warfarin," *Chemosphere*, vol. 34, no. 4, pp. 783–789, 1997.
- [51] L. D. Heimark and W. F. Trager, "The preferred solution conformation of warfarin at the active site of cytochrome P-450 based on the CD spectra in octanol/water model system," *J. Med. Chem.*, vol. 27, no. 8, pp. 1092–1095, 1984.
- [52] P. M. Nowak, F. Sagan, and M. P. Mitoraj, "Origin of Remarkably Different Acidity of Hydroxycoumarins—Joint Experimental and Theoretical Studies," *J. Phys. Chem. B*, vol. 121, no. 17, pp. 4554–4561, May 2017.
- [53] P. Nowak, P. Olechowska, M. Mitoraj, M. Woźniakiewicz, and P. Kościelniak, "Determination of acid dissociation constants of warfarin and hydroxywarfarins by capillary electrophoresis," *J. Pharm. Biomed. Anal.*, vol. 112, pp. 89–97, 2015.
- [54] N. Saleh, M. B. Al-Handawi, M. S. Bufaroosha, K. I. Assaf, and W. M. Nau, "Tuning protonation states of tripeleminamine antihistamines by cucurbit [7] uril," *J. Phys. Org. Chem.*, vol. 29, no. 2, pp. 101–106, 2016.
- [55] B. Valeur and M. N. Berberan-Santos, *Molecular Fluorescence: Principles and Applications*. Weinheim, Germany: Wiley-VCH Verlag GmbH & Co. KGaA, 2012.
- [56] R. Dondon and S. Fery-Forgues, "Inclusion complex of fluorescent 4-hydroxycoumarin derivatives with native  $\beta$ -cyclodextrin: enhanced stabilization induced by the appended substituent," *J. Phys. Chem. B*, vol. 105, no. 43, pp. 10715–10722, 2001.
- [57] P. M. Nowak, F. Sagan, and M. P. Mitoraj, "Origin of Remarkably Different Acidity of Hydroxycoumarins □ Joint Experimental and Theoretical Studies," *J. Phys. Chem. B*, vol. 121, no. 17, pp. 4554–4561, 2017.

- [58] N. Saleh and N. A. Al-Rawashdeh, "Fluorescence enhancement of carbendazim fungicide in cucurbit [6] uril," *J. Fluoresc.*, vol. 16, no. 4, pp. 487–493, 2006.
- [59] R. Badía and M. E. Díaz-García, "Cyclodextrin-based optosensor for the determination of warfarin in waters," *J. Agric. Food Chem.*, vol. 47, no. 10, pp. 4256–4260, 1999.
- [60] J. C. Marquez, M. Hernandez, and F. G. Sánchez, "Enhanced spectrofluorimetric determination of the pesticide warfarin by means of the inclusion complex with  $\beta$ -cyclodextrin," *Analyst*, vol. 115, no. 7, pp. 1003–1005, 1990.
- [61] L. X. Tang and F. J. Rowell, "Rapid determination of warfarin by sequential injection analysis with cyclodextrin-enhanced fluorescence detection," *Anal. Lett.*, vol. 31, no. 5, pp. 891–901, 1998.
- [62] H. C. Hollifield and J. D. Winefordner, "Fluorescence and phosphorescence characteristics of anticoagulants: A new approach to direct measurement of drugs in whole blood," *Talanta*, vol. 14, no. 1, pp. 103–107, 1967.
- [63] A. Abdulmalik *et al.*, "Preparation of soluble stable C60/human serum albumin nanoparticles via cyclodextrin complexation and their reactive oxygen production characteristics," *Life Sci.*, vol. 93, no. 7, pp. 277–282, 2013.
- [64] M. B. Bolattin, S. T. Nandibewoor, S. D. Joshi, S. R. Dixit, and S. A. Chimatadar, "Interaction of hydralazine with human serum albumin and effect of  $\beta$ -cyclodextrin on binding: insights from spectroscopic and molecular docking techniques," *Ind. Eng. Chem. Res.*, vol. 55, no. 19, pp. 5454–5464, 2016.
- [65] J. Chen, C. M. Ohnmacht, and D. S. Hage, "Characterization of drug interactions with soluble  $\beta$ -cyclodextrin by high-performance affinity chromatography," *J. Chromatogr. A*, vol. 1033, no. 1, pp. 115–126, 2004.
- [66] N. Thuaud, B. Seville, A. Deratani, and G. Lelievre, "Determination by high-performance liquid chromatography of the binding properties of charged  $\beta$ -cyclodextrin derivatives with drugs," *J. Chromatogr. A*, vol. 503, pp. 453–458, 1990.
- [67] G. Zingone and F. Rubessa, "Preformulation study of the inclusion complex warfarin- $\beta$ -cyclodextrin," *Int. J. Pharm.*, vol. 291, no. 1–2, pp. 3–10, 2005.
- [68] O. Karadağ, E. Gök, I. S. Ates, Ö. Kiran, and A. Bozkurt, "Inclusion complexation of warfarin with  $\beta$ -cyclodextrins and its influence on absorption

kinetics of warfarin in rat," *J. Incl. Phenom. Mol. Recognit. Chem.*, vol. 20, no. 1, pp. 23–32, 1994.

## Appendix

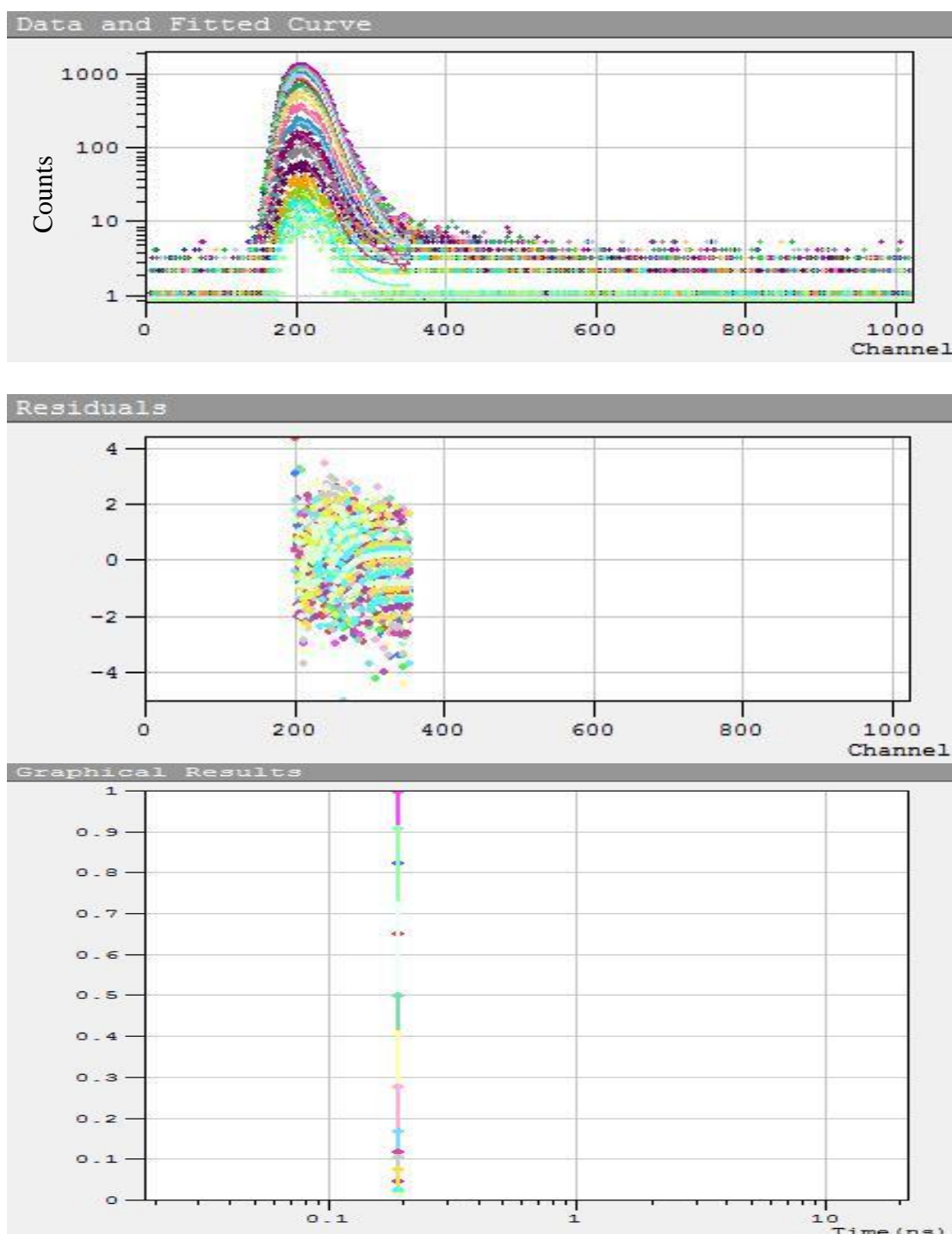


Figure 32: Collected emission decays measured over the emission spectrum of W at pH 3, excited at 320 nm from 330 to 490 nm every 10 nm with a dwell time of 50 s at each wavelength. Data at each wavelength were fitted to a mono-exponential model convoluted with IRF  $\sim 90$  ps (as shown in the residuals)

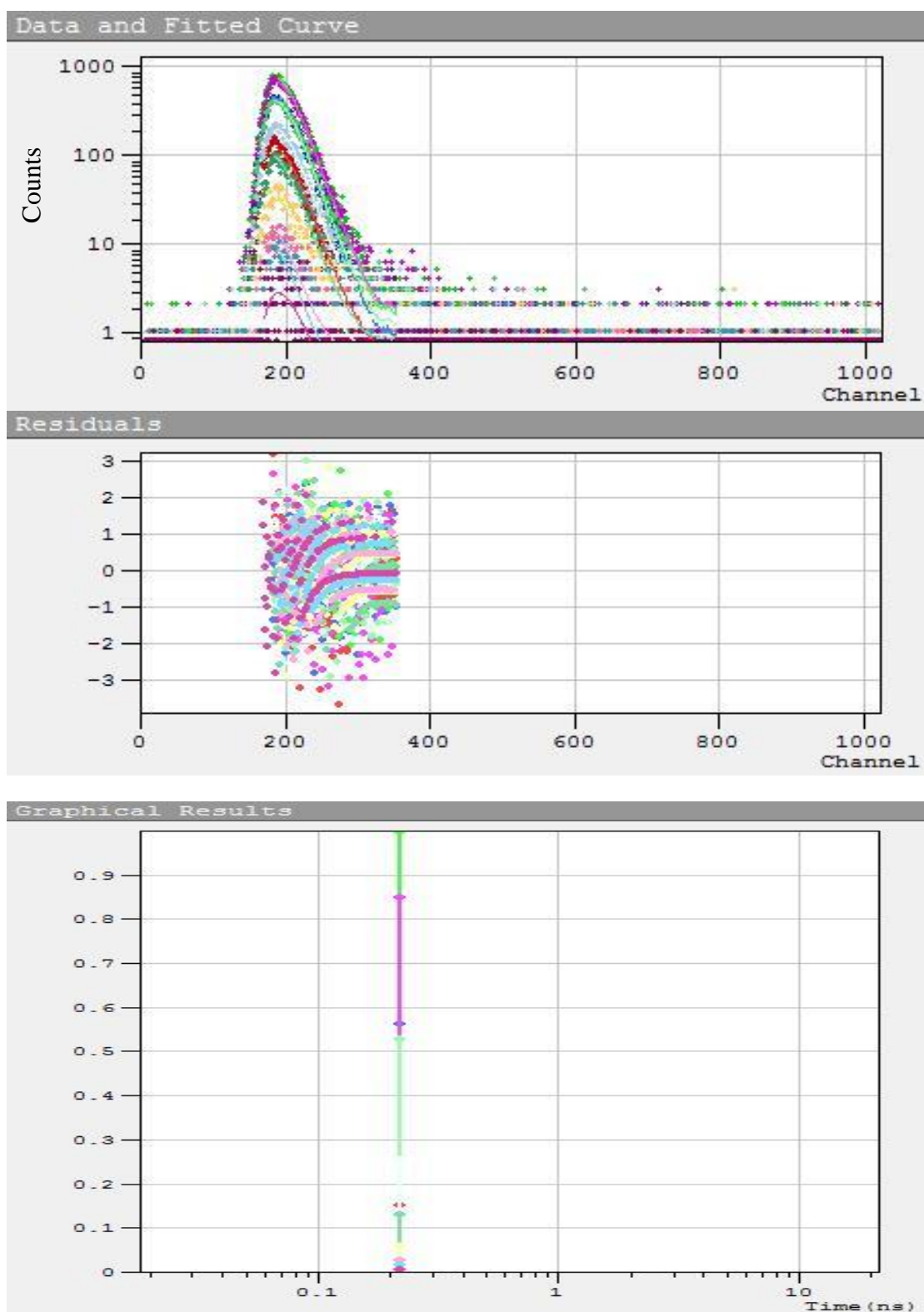


Figure 33: Collected emission decays measured over the emission spectrum of W at pH 3, excited at 280 nm from 310 to 510 nm every 20 nm with a dwell time of 50 s at each wavelength. Data at each wavelength were fitted to a mono-exponential model convoluted with IRF  $\sim 90$  ps (as shown in the residuals)

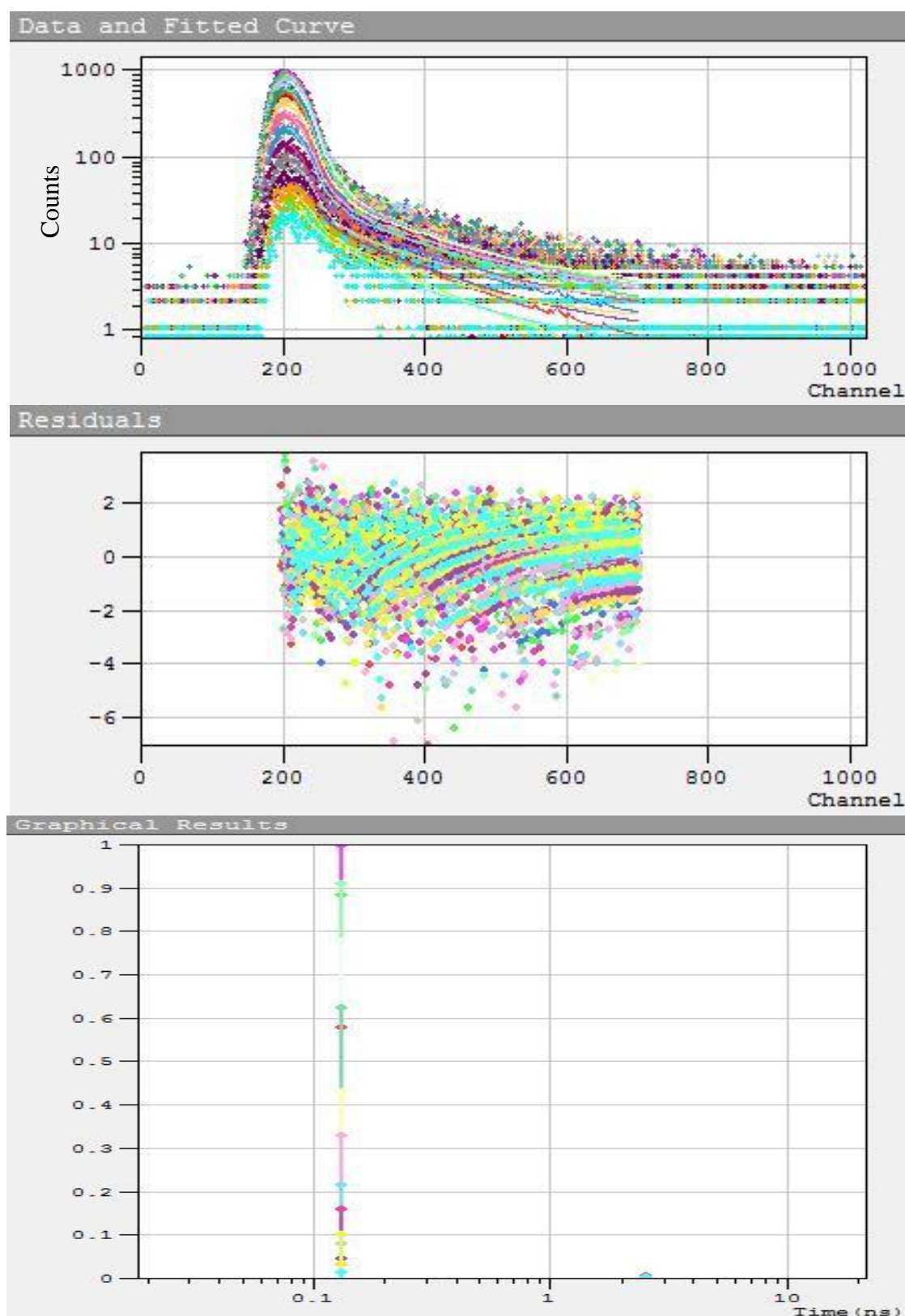


Figure 34: Collected emission decays measured over the emission spectrum of W-Me- $\beta$ -CD at pH 3, excited at 320 nm (Figure 30) from 330 to 480 nm every 10 nm with a dwell time of 50 s at each wavelength. Data at each wavelength were fitted to a bi-exponential model convoluted with IRF  $\sim 90$  ps (as shown in the residuals)

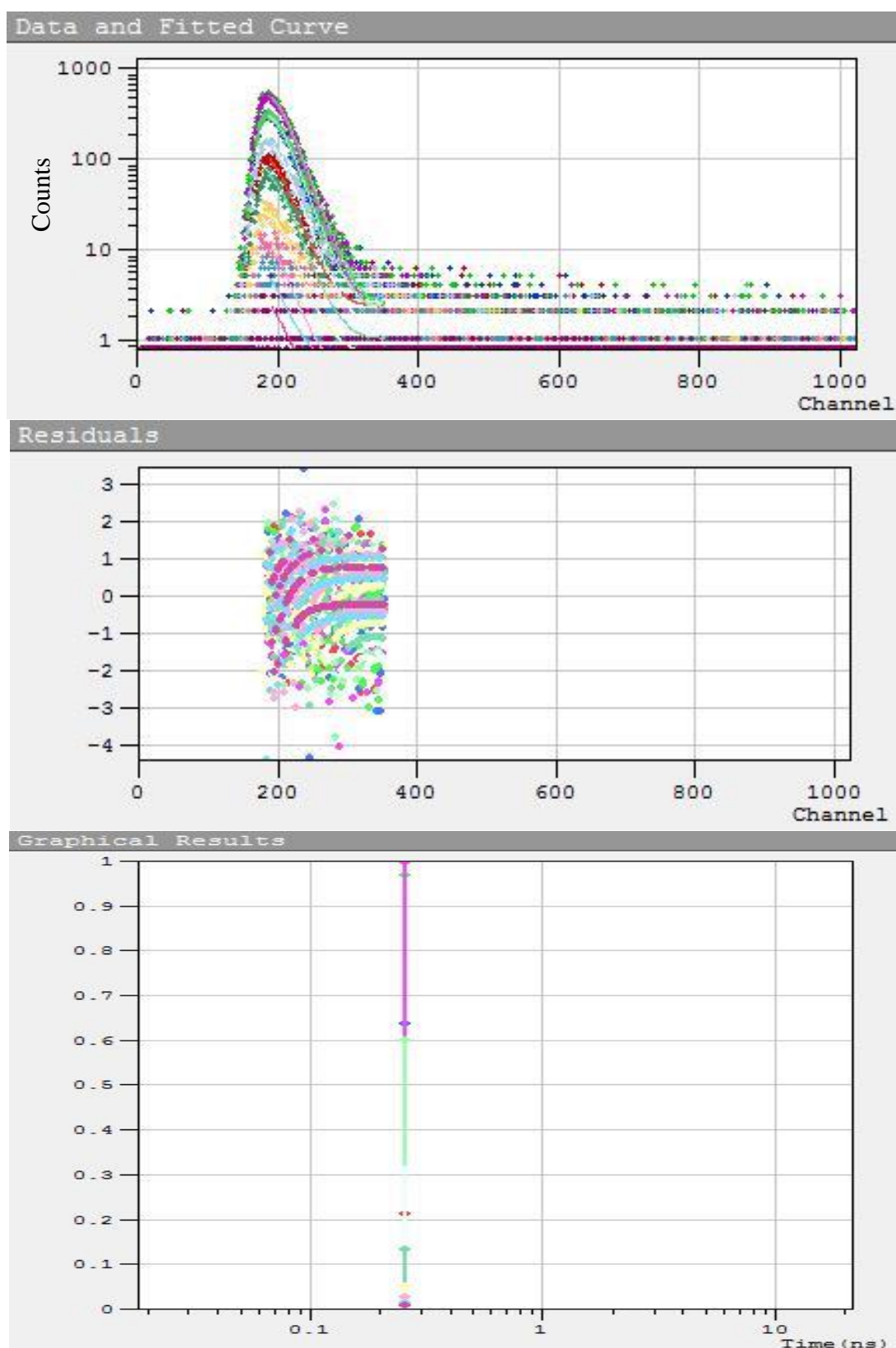


Figure 35: Collected emission decays measured over the emission spectrum of W-Me- $\beta$ -CD at pH 3, excited at 280 nm from 310 to 510 nm every 20 nm with a dwell time of 50 s at each wavelength. Data at each wavelength were fitted to a mono-exponential model convoluted with IRF  $\sim$  90 ps (as shown in the residuals)

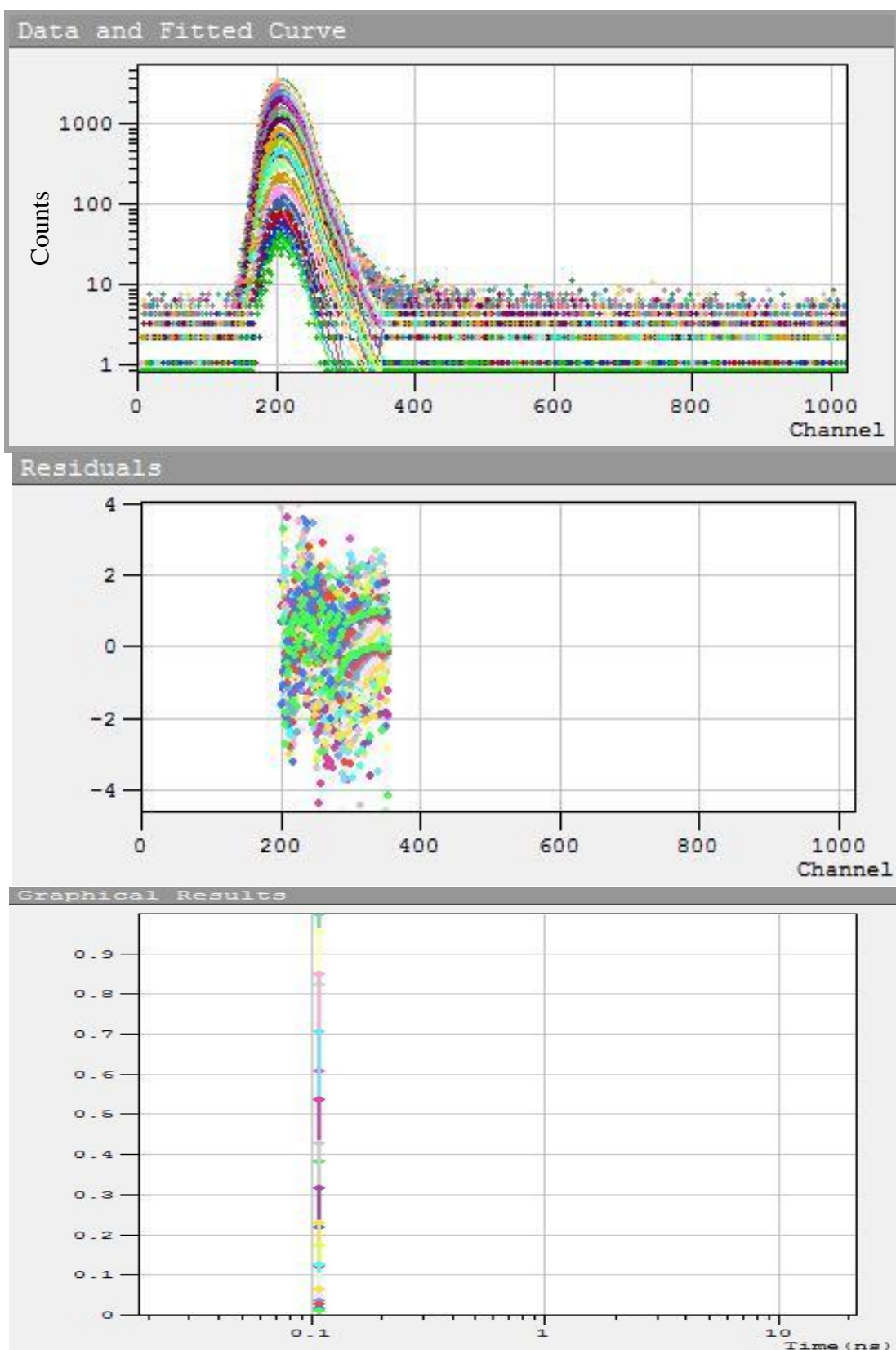


Figure 36: Collected emission decays measured over the emission spectrum of W at pH 9, excited at 320 nm from 330 to 550 nm every 10 nm with a dwell time of 50 s at each wavelength. Data at each wavelength were fitted to a mono-exponential model convoluted with IRF  $\sim$  90 ps (as shown in the residuals)



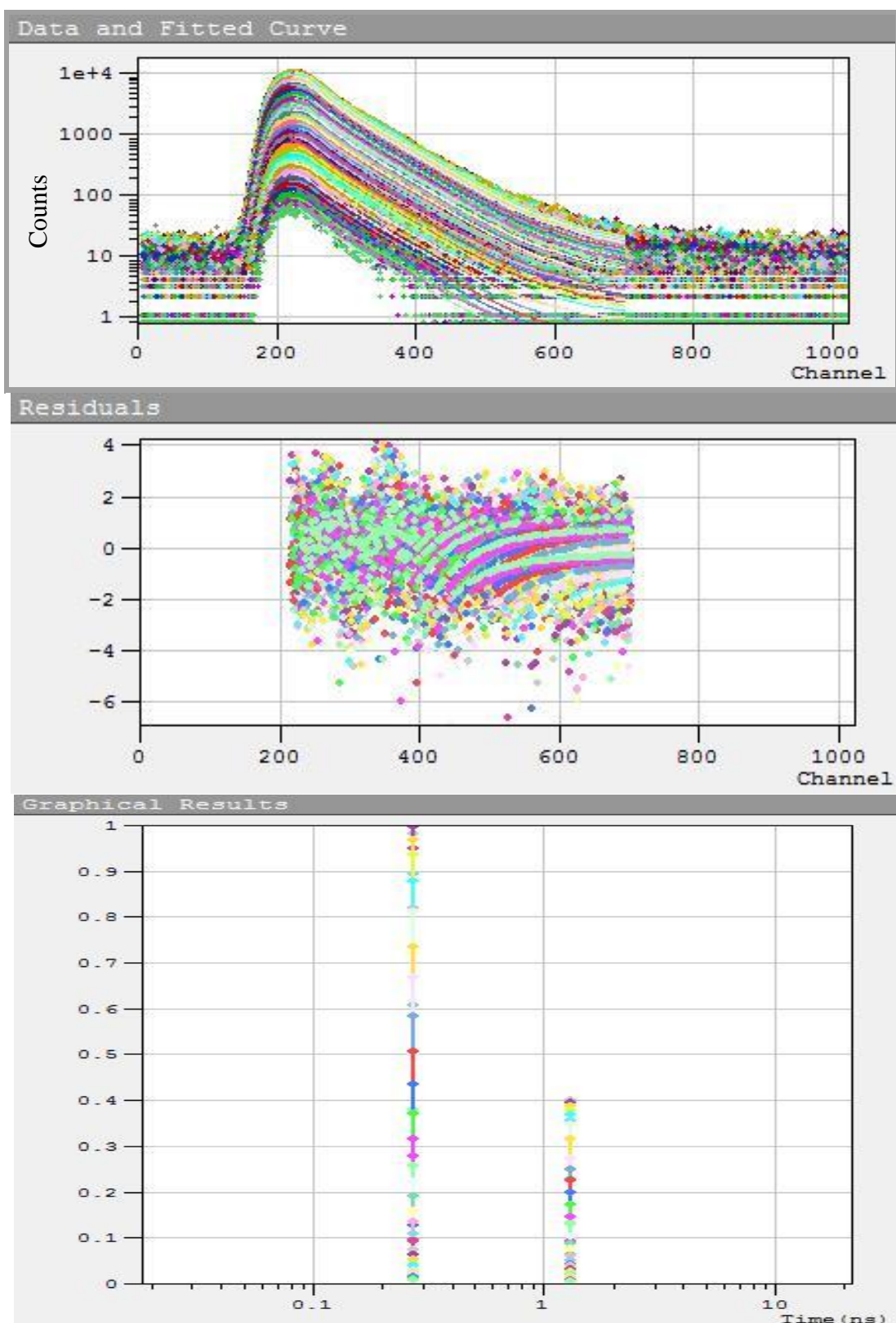


Figure 37: Collected emission decays measured over the emission spectrum of W-Me- $\beta$ -CD at pH 9, excited at 320 nm (Figure 31) from 330 to 550 nm every 5 nm with a dwell time of 50 s at each wavelength. Data at each wavelength were fitted to a bi-exponential model convoluted with IRF~ 90 ps (as shown in the residuals)